ADENINE NUCLEOTIDE TRANSLOCASE AS A REGULATOR OF CHRONIC OBSTRUCTIVE PULMONARY DISEASE AND CYTOSKELETAL FUNCTION

by
Jennifer Nguyen

A dissertation submitted to Johns Hopkins University in conformity with the requirements for the degree of Doctor of Philosophy

Baltimore, Maryland
June 2021

Abstract

Chronic obstructive pulmonary disease (COPD) is characterized by the destruction of alveolar tissue (in emphysema) and airway remodeling (leading to chronic bronchitis) which cause difficulties in breathing. It is a public health concern with few therapeutic options that can reverse disease progression or mortality. This is in part because current treatments mainly focus on ameliorating symptoms induced by inflammatory pathways as opposed to curing disease. Hence, emerging research focused on upstream pathways are likely to be beneficial in the development of efficient therapeutics to address the root causes of disease. Because of the complexity of COPD and unknown targets for disease onset, simpler model organisms have proven to be useful tools in identifying disease-relevant pathways and targets. Here, we share results from a study that utilized a high-copy cDNA library genetic selection approach in *Dictyostelium discoideum* to identify protectors against cigarette smoke. Adenine nucleotide translocase was found to be protective against cigarette smoke in both *Dictyostelium* and human bronchial epithelial cells. We highlight that ANT defends against cigarette smoke by modulating metabolic activity and airway function. Interestingly, this work facilitates the interplay between metabolism and cytoskeletal function. We also share an exploration of the feedback between ANT and key players in cell mechanics. Overall, ANT being a modulator of metabolism, airway integrity, and cell shape change in the context of COPD makes it a potential therapeutic target to treat the disease.

Primary Reader and Advisor: Douglas N. Robinson, Ph.D.

Secondary Reader: Venkataramana K. Sidhaye, M.D.

Acknowledgements

First, I would like to thank Doug for his mentorship during my time at Hopkins. He provided helpful guidance as I learned how to think critically and tried to solve challenging scientific questions. I appreciate that he encourages everyone in his lab to explore their scientific interests, including through exposure to research at national meetings and local conferences. He also takes the time to see that everyone in his lab improves professionally by coaching us on how to present talks and how to write grants. He has certainly contributed to my improvement in presenting and creating talks, and I know that these skills will continue to be useful for me in my future endeavors. Doug cares for everyone in his lab, and he has built a welcoming and supportive environment. I am certainly appreciative of the strong camaraderie amongst the Robinson lab members.

And with that, I would also like to thank the members of the Robinson lab, past and present, for their support. I want to give special thanks to Alexandra, Priyanka, Eric, Dustin, Eleana, Yinan, Ly, Mengni, Amanda, Laura, Corrine, Cathy, Mark, Shantel, Kat, and Brian. I feel like I grew as a scientist because of their constructive advice and questions. Everyone also made the lab an entertaining and warm environment. I enjoyed the times we had lunch together and talked about science and life. I gained confidence in myself with the help of my lab mates and appreciated having strong female mentors in the lab who have inspired me. I would also like to thank my thesis committee members, Ramana Sidhaye, Steve Claypool, and Jun Liu, for giving me helpful feedback for my project. I also greatly appreciate the support from Caren Meyers, the Pharmacology Graduate Director, for her encouragement over the years. I also want to thank my friends, peers, and classmates in the Pharmacology program. I am thankful for their support as we made it through the first two years of classes and oral examinations together. Exploring Baltimore has also been a lot of fun with you all.

I want to thank Kyle Baeta-Orick, who has supported me near the end of my graduate school journey. He has been really encouraging and a great support system especially during the events of 2020. Finally, I would like to thank my family including my sister, Tracy, my mom, Michelle, my stepdad, Vu, and my dad, Long. Being far away from them after college has been difficult, but they have always been supportive of me throughout my life. I appreciate that they continue to encourage me to try my best, and I definitely contribute making it this far to them.

Table of Contents

List of Tables

List of Figures

Chapter 1: Introduction

Chronic obstructive pulmonary disease (COPD), an illness that diminishes lung function to make breathing difficult, is one of the leading causes of death in the United States and worldwide (Lopez-Campos et al., 2016; Xu et al., 2020). An estimated 328 million people have COPD worldwide as of 2010, and COPD is predicted to be the third leading cause of death in the world by 2030 (Lopez-Campos *et al.*, 2016). Considering its impact on public health, research on what underlies COPD for the development of therapeutics has been underway for decades. Nonetheless, COPD continues to have a lack of therapeutic options that can reverse lung damage and prevent disease progression. Although research on COPD is ongoing and new therapeutics are currently in the pipeline, there continues to be few advances on the root causes of the disease and potential treatments to stop them. Here, I will include a general overview of COPD pathology and some of the therapeutic strategies currently in use. In addition, I will discuss emerging COPD research that has the potential to provide new breakthroughs for therapeutic development.

General pathology and treatment of stable COPD

A major cause of COPD is exposure to tobacco smoke. Continual exposure to the compounds in tobacco smoke induces tissue damage and inflammatory responses that lead to the primary phenotypes of the disease: emphysema and chronic bronchitis. Emphysema is characterized as the destruction of alveolar tissue. As a result, lung elasticity is lost by the degradation of the extracellular matrix (ECM) and alveolar cells are lost through apoptosis and autophagy (Tuder and Petrache, 2012). Apoptosis, inflammation, and ECM breakdown continue to propagate in self-amplifying loops that further the progression of emphysema (Tuder and Petrache, 2012). In the airways, inflammation can occur in both the large and small airways after exposure to tobacco

smoke. Chronic smoking also increases the chances of remodeling of the airways (Tuder and Petrache, 2012). Airway remodeling, the overproduction of mucus by airway goblet cells, and the increased difficulty in airway clearance contribute to airflow obstruction found in chronic bronchitis (Kim and Criner, 2013). One of the detriments of COPD is that the disease progresses even after smoking cessation (Tuder and Petrache, 2012).

The 2020 Global Initiative for Chronic Obstructive Lung Disease offers recommendations for pharmacological COPD treatment based on patient symptoms and history of hospitalizations. Patients with mild COPD are generally given short-acting or long-acting β_2-agonists and/or anti-muscarinic drugs (Global Initiative for Chronic Obstructive Lung Disease, 2020). β_2-agonists stimulate β_2-adrenergic receptors, leading to increased cAMP levels and protein kinase A activation (Global Initiative for Chronic Obstructive Lung Disease, 2020). Anti-muscarinic drugs block acetylcholine from binding to muscarinic receptors in the smooth muscle of the airways (Global Initiative for Chronic Obstructive Lung Disease, 2020). Through these mechanisms, both types of drugs reduce bronchoconstriction in airway smooth muscle. If symptoms worsen, inhaled corticosteroids can be used in combination with long-acting β_2-agonists or anti-muscarinic drugs that treat dyspnea and exacerbations (Global Initiative for Chronic Obstructive Lung Disease, 2020). Other options available for more severe cases of COPD include the PDE4 inhibitor, roflumilast, in combination with the drugs stated previously (Calverley et al., 2009). Current treatments for COPD mainly focus on addressing the symptoms of the disease, and evidence also suggests that some patients are resistant to inhaled corticosteroid treatment (Calverley *et al.*, 2009). With the limitations of current treatments, more effective treatment strategies are needed. One potential strategy includes implementing a precision medicine approach that identifies

more upstream cellular and molecular pathways undermining the disease (Sidhaye et al., 2018).

Recent COPD pipeline strategies

In lieu of developing more disease-specific treatments, we describe some current efforts by other groups in the COPD pipeline to address disease onset (**Figure 1.1**). These efforts are heavily focused on targeting inflammatory pathways, which is relevant considering that inflammation is one of the main contributors to disease pathology. Nonetheless, inflammation in COPD is complex and involves a host of pathways (Barnes, 2016a). Therefore, targeting only one pathway may not necessarily be effective in treating COPD. In fact, several drug development strategies have failed to show efficacy possibly due to this issue. Delivery strategies may also contribute to this lack of efficacy. Oral drugs can cause off-target effects as they do not directly encounter the airways as efficiently as inhaled medications. Nevertheless, the following describes some significant players in COPD and promising targets that can address inflammatory complications.

Oxidative stress

Oxidative stress is thought to be a significant driver of COPD as several disease-related pathways are affected, including inflammation, aging, and DNA damage (Barnes, 2020). While oxidative stress impacts many pathways, one that is well-studied involves Nrf2, a transcription factor, and its interaction with the negative regulator, Kelch-like ECH-associated protein 1 (KEAP1). Oxidative stress inactivates KEAP1, allowing Nrf2 to translocate into the nucleus where it activates pathways that increase antioxidant metabolism and attenuate inflammatory responses (Cuadrado et al., 2019). In the context of COPD, Nrf2 activity increases with cigarette smoke (CS) exposure due to the

increase in oxidative stress, but its activity declines with the progression of COPD (Sidhaye et al., 2019). In a study with a small group of COPD patients, gene expression levels downstream of Nrf2 were higher in bronchial epithelial cells of current smokers versus former smokers, consistent with Nrf2-related anti-inflammatory activity occurring

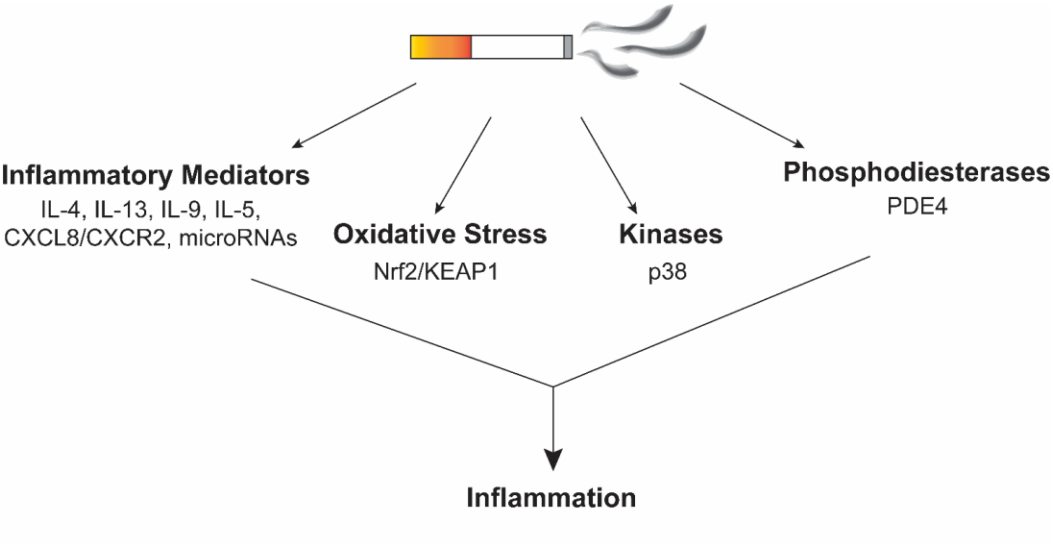

Figure 1.1. The COPD pipeline focuses on targeting inducers of inflammation. Cigarette smoke activates numerous downstream pathways and targets that lead to inflammation including inflammatory mediators, oxidative stress, kinases, and phosphodiesterases. Current therapeutic strategies aim to reduce inflammatory responses by inhibiting specific targets under each major group.

with CS exposure (Sidhaye *et al.*, 2019). CS extract (CS bubbled into cell media) also affects Nrf2 activity in differentiated primary normal human bronchial epithelial cells (NHBE) grown at air-liquid interface. Several oxidative stress responsive genes related to the Nrf2 pathways are upregulated with CS extract exposure (Sekine et al., 2019). In addition, Nrf2 protein expression has a biphasic relationship with CS extract exposure, increasing then decreasing with increased concentrations of CS extract (Sekine *et al.*, 2019). This result supports the idea that Nrf2 is important in regulating inflammatory responses from CS initially, but loses this ability with continual exposure to CS.

Many lines of evidence implicate Nrf2 in COPD pathology; thus, Nrf2 and its associated signaling pathways are being pursued as therapeutic targets. One study identified the Receptor for Advanced Glycation End Products (RAGE), a member of the immunoglobulin superfamily, as a deactivator of Nrf2 activity in response to CS exposure (Lee et al., 2018). An antagonist for RAGE, FPS-ZM1, promoted Nrf2 translocation into the nucleus, allowing for decreased expression of damage-associated-molecular-patterns signaling (Lee *et al.*, 2018). Other agents that change Nrf2 expression and activity in airway cells include aspirin-triggered resolvin D1, crocin, sulforaphane, and schisandrin B (Dianat et al., 2018; Jia et al., 2017; Jiao et al., 2017; Posso et al., 2018). Sulforaphane, a natural compound found in cruciferous vegetables that activates Nrf2 by binding to KEAP1, proceeded into clinical trials for a variety of diseases (Cuadrado *et al.*, 2019). Nonetheless, in a trial for COPD, sulfurophane failed to show efficacy because Nrf2 gene expression and inflammatory markers levels did not consistently change after treatment in both alveolar macrophages and bronchial epithelial cells (Cuadrado *et al.*, 2019). This result is possibly due to poor drug penetration to the lung (Barnes, 2020). Something else to note is that this trial measured these parameters after a few weeks of treatment instead of a longer period of time (Wise et al., 2016). Other COPD drugs in the pipeline are non-electrophilic non-covalent drugs that target the Nrf2-KEAP1 protein-protein interaction rather than the proteins themselves (Cuadrado *et al.*, 2019). Non-electrophilic PPI inhibitors have different pharmacodynamics and off-target effects compared to electrophilic drugs like sulforaphane, thus offering another avenue for drug development on Nrf2 (Cuadrado *et al.*, 2019).

Kinase-mediated pathways

Several types of kinases induce chronic inflammation when activated, making them another therapeutic target group for COPD (Barnes, 2016b). Indeed, drugs have

been, or currently are in development that target a variety of kinase groups, including MAPK, receptor-tyrosine kinases (RTK), phosphoinositide-3-kinases (PI3Ks), JAK, and NF-κB (Barnes, 2016b). However, none have been approved for clinical use possibly due to issues such as target specificity and loss of efficacy over time (Barnes, 2016b). For instance, one group that drew attention for clinical development was the p38 MAPK family. Inhibiting p38 reduces inflammation in cellular and animal models, but many failed to show promise in clinical trials (Barnes, 2016b). An example is the p38α compound AZD7624, which decreases cytokine release in human alveolar macrophages but did not decrease exacerbations in COPD patients (Patel et al., 2018). However, work on developing and studying more specific inhibitors are underway. One such p38 inhibitor with evidence of efficacy is RV-568. Classified as a narrow-spectrum kinase inhibitor with high potency for the α and γ isoforms of p38, RV-568 demonstrated anti-inflammatory activity in monocytes, macrophages, and epithelial cells by inhibiting cytokine (CXCL8 and IL-6) release (Charron et al., 2017). Animal models also showed promising results, and in a small 14-day clinical trial, lung function improved with drug treatment (Charron *et al.*, 2017).

Phosphodiesterase inhibitors

Interest in phosphodiesterase 4 (PDE4) inhibitors arose with the discovery that increasing intracellular cAMP levels can have anti-inflammatory effects. PDE4 subtypes are found in various immune cells and cells affected by immune response (Sakkas et al., 2017). When they are inhibited, cAMP signaling allows for the upregulation of cAMP-response element (CRE)-containing genes and the inhibition of NF-κB, which decreases inflammatory responses (Sakkas *et al.*, 2017). The consequences of decreased cAMP via PDE upregulation can occur in airway cells and lung tissue as well. In a study with precision lung slices from CS-exposed mice, intracellular cAMP levels are decreased

based on FRET sensor measurements (Zuo et al., 2018). Protein and mRNA levels are lower for two paralogs of PDE4 (PDE4B, PDE4D; two of the four PDE4 genes) in these animals as well (Zuo *et al.*, 2018). In another study by authors in the same group, they discovered that among patients, smokers have increased protein expression of PDE4D in the airway epithelium (Zuo et al., 2020). These works highlight PDE4 as a candidate for drug development against CS-induced inflammation.

As mentioned above, the PDE4 inhibitor roflumilast is used for more severe cases of COPD (Global Initiative for Chronic Obstructive Lung Disease, 2020). Nevertheless, its efficacy is limited due to it being an oral drug and causing adverse side effects. Hence, more potent analogs of roflumilast are being developed (Moussa et al., 2018). Several inhaled formulations of PDE4 inhibitors are in the pipeline too, which may improve their efficacy compared to roflumilast (Phillips, 2020). One of these drugs, CHF6001 showed promise in clinical trials by decreasing the inflammatory biomarkers LTB4, CXCL8, MMP9, TNFα, and MIP-1β in sputum of patients already on triple therapy with inhaled β_2-adrenergic agonists, anti-muscarinics, and inhaled corticosteroids (Singh et al., 2019). Similar results appeared in alveolar macrophages and lung tissue from COPD patients with CHF6001 reducing TNFα production (more potently than roflumilast) and activating CREB (Lea et al., 2019).

Another drug in clinical trials is ensifentrine/RPL554, a dual PDE3/PDE4 inhibitor. In addition to having anti-inflammatory effects, ensifentrine invokes bronchodilator effects (Singh et al., 2018). Ensifentrine also improves the effects of other bronchodilators when they are used in combination (Singh *et al.*, 2018). The forced expiratory volume (volume of air forcefully expelled) in one second, or FEV_1, increases with ensifentrine together with salbutamol (β_2-adrenergic agonist), or ipratropium (anti-muscarinic), both short-acting bronchodilators, than each short-acting bronchodilator alone (Singh *et al.*, 2018). Ensifentrine with tiotropium, a long-acting bronchodilator with

anti-muscarinic effects, demonstrated similar benefits in FEV_1 (Singh *et al.*, 2018). More clinical trials are planned for ensifentrine, and other PDE4 inhibitors continue to be in the pipeline as well (Singh *et al.*, 2018).

Inflammatory mediators

Interleukins serve as inflammatory mediators, and variants such as IL-4, IL-13, IL-9, and IL-5, which promote type 2 immunity, have been implicated in COPD disease progression (Barnes, 2018). Interleukins are released from a variety of cell types from exposure to tobacco smoke or other inhaled irritants. Aside from immune cells, tobacco smoke can cause epithelial cells, endothelial cells, and fibroblasts to release these mediators (Barnes, 2016a). The mediators then increase the number of macrophages, neutrophils, eosinophils, lymphocytes, dendritic cells, and other immune cells that induce inflammatory responses (Barnes, 2016a).

Targeting these interleukins is of interest for developing therapeutics because of their role in promoting inflammatory responses. In a recent study, the authors found that IL-4, in an elastase-induced emphysema mouse model, is released from basophils and promotes alveolar destruction by increasing metalloproteinase-12 expression (Shibata et al., 2018). Another study demonstrated that IL-9 inhibition in a COPD mouse model also abrogates structural damage from CS exposure (Zou et al., 2018). In terms of drug development, IL-5 and its receptor IL-5Rα, key players in eosinophil-related inflammation, are targets of blocking antibodies mepolizumab, reslizumab, and benralizumab (Barnes, 2018). These drugs are approved for asthma but failed to show improved efficacy in COPD clinical trials (Barnes, 2018). Nonetheless, these drugs have not yet been tested for efficacious effects in COPD patient subgroups with eosinophilia. Other approved drugs for asthma target IL-13 and IL-4, but these drugs have not been extensively tested for COPD treatment. Clinical trials are still open for such studies with

dupilumab, an IL-4 and IL-13 receptor monoclonal antibody, being a candidate (Barnes, 2018).

Despite the interest in developing compounds for eosinophilic inflammation, research is ongoing to elucidate the effects of other inflammatory mediators on disease progression. Higher concentrations of cytokines, such as TNFα, exist in sputum and exacerbations of COPD patients (Barnes, 2018). IL-17 appears to have a role in small airway fibrosis in COPD model mice, and metalloproteinases (MMPs), particularly MMP-9, are also targets of interest due to their involvement in alveolar wall destruction (Barnes, 2016a; Yanagisawa et al., 2017). Chemokines are also generating interest with CXCL8 and its receptor CXCR2 being the major targets. Interestingly, microRNAs, which likewise regulate inflammation, are involved in COPD with miR-155 expression being increased in COPD patients compared to nonsmokers (De Smet et al., 2020). MiR-155 knockout mice have lower levels of inflammatory markers and cells, and elastase-induced emphysema is attenuated in these mice. No miRNA-based therapeutics for COPD exist yet, although they have utility in diseases like cancer (Hanna et al., 2019).

Opportunities for new breakthroughs

Many of the current drug development strategies for COPD focus on targeting pro-inflammatory pathways. While these strategies are helpful in treating inflammation, lung damage remains and continues to be irreversible. Hence, there is a need for research into areas that have the potential to address these issues such as how lung damage occurs further upstream of inflammation. Delving into these upstream pathways may offer more potential therapeutic targets that may address the root causes of disease (**Figure 1.2**). In addition, conducting research on lung repair and regeneration may present other useful strategies to counter damage already done to the lung.

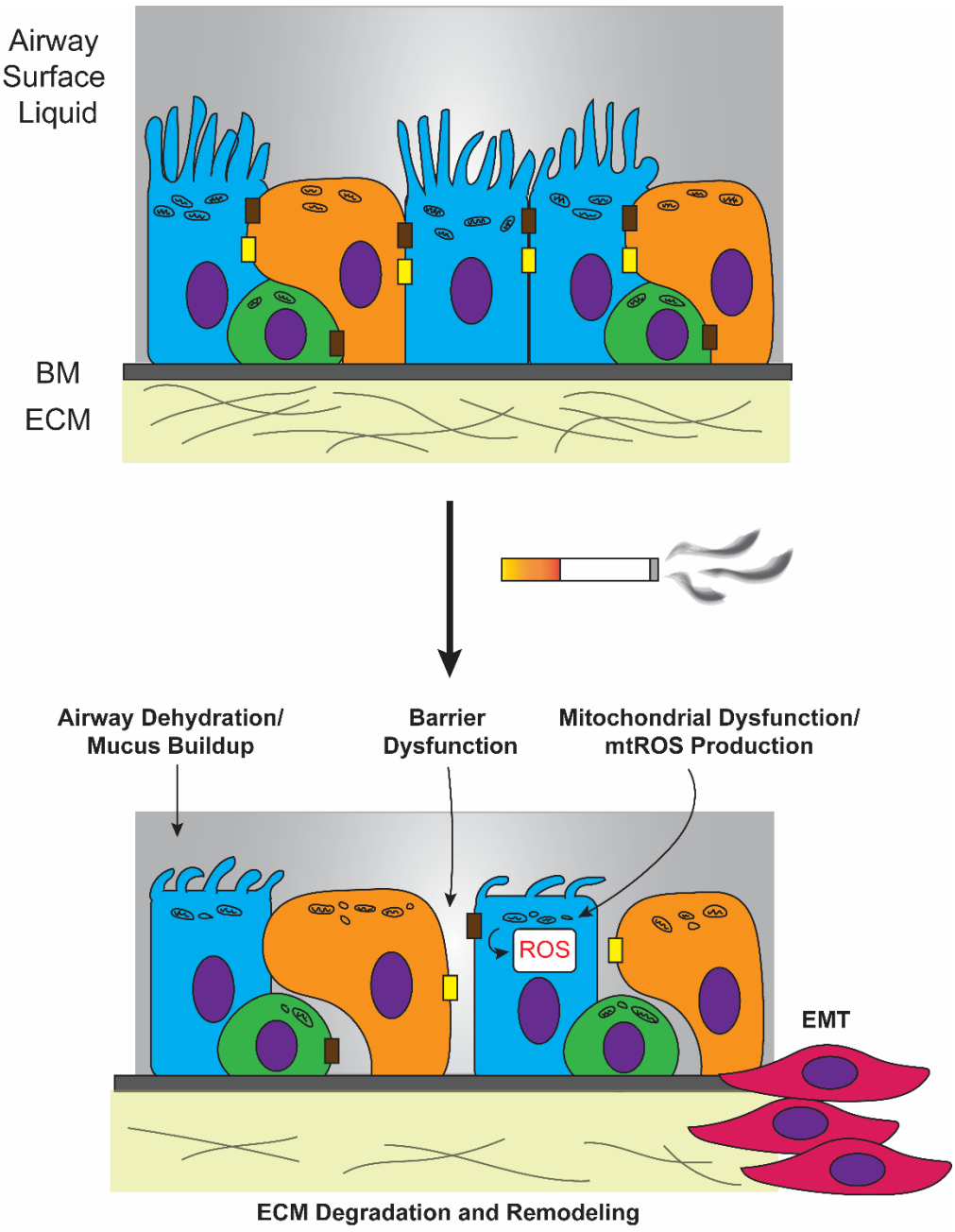

Figure 1.2. Emerging COPD biology offers potentials for new breakthrough in therapeutic development. The airway epithelium is composed of ciliated cells (blue), secretory cells (orange), and basal cells (green) on top of a basement membrane (BM) and extracellular matrix (ECM). Its role is to act as a barrier to toxins that enter in the airway including cigarette smoke. Continual exposure to cigarette smoke in the epithelium, however, can contribute to COPD phenotypes. Pathways that are affected by cigarette smoke upstream of inflammatory responses are currently being researched and may be helpful in identifying new targets for drug development. These pathways include airway hydration, the structural integrity of the airway epithelium and its barrier function, mitochondrial dysfunction and mtROS production, extracellular matrix remodeling, and epithelial-to-mesenchymal transition (EMT).

Uncovering new methodologies to assist in conducting these new areas of research could also be of interest. For example, model organisms can help to identify new disease-relevant targets. These targets or other pathways implicated in COPD can be further studied in human cellular disease models, which are also being currently researched and developed. More comments on these points and information on ongoing research are briefly described below.

Mitochondria

Mitochondria are a major source of endogenous reactive oxygen species (ROS) when under stress, making them viable targets for therapeutic research. Studies have focused on how mitochondrial dysfunction arises in the context of COPD and CS exposure (Aghapour et al., 2020). Many of these findings suggest that mitochondrial morphology, metabolism, and other functions become abnormal in human and mouse airway epithelial cells from CS. More recent findings highlight the effects of CS on mitochondrial morphology and the impact of these morphological changes. In human airway smooth muscle cells, CS causes mitochondrial fragmentation by decreasing expression of mitochondrial fusion protein, Mfn2, and increasing expression of fission protein, Drp1 (Aravamudan et al., 2017). This fragmentation leads to loss of mitochondrial membrane potential and defects in oxidative phosphorylation (Aravamudan *et al.*, 2017). Interestingly, CS induces proliferation and airway remodeling in these cells, suggesting that the promotion of mitochondrial fission drives cells towards glycolysis for energy (Aravamudan *et al.*, 2017). Similarly, in primary human alveolar type II cells from smokers and patients with emphysema, mitochondrial membrane potential and mtDNA repair are disrupted, leading to higher mtDNA damage, along with decreased mitochondrial fission (Kosmider et al., 2019).

Other proteins of interest affected by CS that contribute to mitochondrial dysfunction in the airway epithelium include Miro1, Nix, and pp66Shc. The expression levels of Miro1, a GTPase that is involved in mitochondrial shape and trafficking, are reduced after exposure to CS extract. Decreases in Miro1 cause defects in mitophagy, an important process in removing damaged mitochondria (Sundar et al., 2019). In the same vein, increases in Nix levels by CS extract induce mitophagy. Nix is involved in mitochondrial clearance and is related to the pro-apoptotic BH3-only proteins. When it is silenced by siRNA, CS extract-induced defects in ATP levels and mitochondrial membrane potential are ameliorated (Zhang et al., 2019). Finally, pp66Shc is an adaptor protein that is translocated into the mitochondria and generates ROS when phosphorylated by protein kinase C (PKC) isozymes. In airway epithelial cells exposed to CS extract, pp66Shc expression increases, resulting in increased mitochondrial ROS production (Zhang et al., 2018). Interestingly, pp66Shc silencing attenuates this effect on ROS and improves other mitochondrial processes (Zhang *et al.*, 2018). Considering how involved these proteins are in mitochondrial injury, they can be potential therapeutic targets against mitochondrial-induced ROS. The pathways and processes related to these proteins (mitophagy, oxidative phosphorylation, fusion/fission) may also be valuable to examine further to identify additional targets to reduce the impact of ROS.

Structural integrity of airway epithelium

The airway epithelium is the first line of defense against any particulates and bacteria that enter the airway, yet this epithelium must maintain a barrier that is selectively permeable. Toxins such as CS can interrupt this barrier function, leading to the release of inflammatory signals that contribute to the onset of disease (Aghapour et al., 2018). On a mechanistic level, one reason for the loss of monolayer integrity is the disruption of cellular junctions. Proteins that comprise tight junctions (such as ZO-1 and

occludins) or adherens junctions (like E-cadherin) are downregulated in airway cells exposed to CS, resulting in a loss in barrier function reflected by a decrease in transepithelial resistance (Aghapour *et al.*, 2018). Investigations into therapeutic compounds that target junctional proteins are underway, but they are still limited (Aghapour *et al.*, 2018).

To further understand barrier function in a related context, studies on cell mechanics and the cytoskeletal elements that interact with these junctions are transpiring. The actin cytoskeleton, which is linked to apical tight junctions and regulates cell structure, is affected by continual CS exposure in NHBEs (Aghapour *et al.*, 2018). Actin assembly increases with more CS exposure, and cortical tension, a measure of cell stiffness, also rises (Nishida *et al.*, 2017). Increased actin polymer levels and cell stiffness may contribute to the tissue remodeling and barrier dysfunction seen in COPD (Nishida *et al.*, 2017). Indeed, other studies are emerging on actin and actin-associated proteins as potential regulators of disease. A study identified other actin-related proteins affected by CS via mass spectrometry: coactosin-like protein (COTL1), microtubule-associated protein RP/EB family member 1 (MARE1), and heat shock protein B1 (HSPB1) (D'Anna et al., 2017). Another identified potential protein affected by CS is the family-with-sequence-similarity-member-13A (FAM13A), a modulator of RhoA activity and actin dynamics (Castaldi et al., 2019). Rac1, a regulator of actin assembly, is also implicated in epithelial-to-mesenchymal transition (EMT) (Jiang et al., 2017). EMT, the process of the airway epithelium becoming more mesenchymal, is also thought to occur in COPD (Aghapour *et al.*, 2018). Many proteins feed into this process, and future studies may reveal several cytoskeletal proteins as key players of EMT during COPD.

The extracellular matrix (ECM) is an additional structural component of the airway epithelium that likely contributes to COPD phenotypes. In epithelial and alveolar cells, the breakdown of the ECM by proteases such as MMP-9 is presumed to help

cause emphysema by inducing inflammatory responses and airway remodeling (Aghapour *et al.*, 2018). Indeed, the concentrations of biomarkers indicating ECM degradation for components like elastin, collagen I, and collagen IV, are higher in COPD patients as compared to healthy patients (Bihlet et al., 2017). Interestingly, when NHBEs are grown on a scaffold containing ECM from COPD patients, expression for COPD-related genes is altered in these cells as compared to those grown on scaffolds from healthy patients (Hedstrom et al., 2018). The various changes in gene expression point towards a COPD phenotype, suggesting that changes in the ECM can disrupt the integrity of the airway epithelium (Hedstrom *et al.*, 2018). While previous studies have attempted to develop therapeutics against the proteases (MMPs, etc.) that degrade the ECM, they have been unsuccessful in procuring an effective drug. Other proteins, such as cytoskeletal proteins that regulate the ECM, may be valuable targets. For example, defects in non-muscle myosin II (NM II), a force-generating motor protein important in cell structure and shape change, altered ECM remodeling in a mouse model and induced an emphysema-like phenotype (Kim et al., 2018). With modulators against some isoforms of NM II already discovered like 4-hydroxyacetophenone (4-HAP), they may be interesting candidates to test in therapeutic studies (Surcel et al., 2015).

Airway hydration

In addition to being a barrier that prevents bacteria and particulates from entering the airway, the epithelium functions to trap these particulates and remove them from the airway altogether. Mucus produced by goblet cells is released on the surface of the airway forming a layer of apical liquid called the airway surface liquid (ASL), which includes a mucus layer and an aqueous periciliary layer. Mucociliary clearance is propagated by motile cilia along the surface of the epithelium (Ghosh et al., 2015). CS appears to affect mucociliary clearance by shortening cilia length, slowing down ciliary

beating, increasing mucus secretion, and lowering ASL height (Ghosh *et al.*, 2015). This reduction in mucus clearance causes mucus build-up, which can be one of the causes of airway obstruction and infection found in chronic bronchitis (Ghosh *et al.*, 2015). Cystic fibrosis (CF) comparably occurs from reduced airway hydration and lack of mucus clearance, making therapeutic targets from CF potentially useful for COPD treatment. Interestingly, CFTR, an anion channel that secretes Cl^- to maintain airway hydration, is affected by CS exposure in human bronchial epithelial cells with a recent study by Marklew *et al*. suggesting CS leads to its inactivation by internalization trafficking (Marklew et al., 2019). Overall, CFTR and other ion channels, like the epithelial sodium channel (ENaC), that are responsible for airway hydration may be helpful targets to pursue and studies on their therapeutic potential are ongoing (Ghosh *et al.*, 2015; Moore et al., 2018).

Pro-regenerative strategies

The progression of COPD disrupts repair mechanisms, resulting in irreversible lung damage. This observation has generated an interest in regenerative strategies such as stem cell and tissue-engineering treatments to repair areas of the lung that are already damaged. One extensively studied method is the infusion of mesenchymal stromal cells (MSC) at sights of injury. Interestingly, MSCs demonstrated anti-inflammatory effects and induced paired in *in vitro* and *in vivo* mouse models, but clinical trials with MSCs have yet to show efficacy (Sun et al., 2018). MSCs did not affect pulmonary function or quality of life in these trials (Sun *et al.*, 2018). Nonetheless, making changes to MSC clinical trial design and conducting more studies to understand how MSCs work mechanistically may address the disparity between the preclinical and clinical trial data.

Another therapeutic approach is to target and activate endogenous regenerative mechanisms in the lung that are affected by COPD. Most studies on lung regeneration have been conducted in mouse models, and they have procured relevant pathways, including Wnt/β-catenin, Notch, Fibroblast Growth Factor (FGF), retinoic acid (RA), and Hedgehog signaling (Ng-Blichfeldt et al., 2019). Interestingly, Wnt and Notch signaling are both disrupted in airway epithelial cells of COPD patients (Ng-Blichfeldt *et al.*, 2019). Gene expression for proteins related to RA transport and activity are altered in COPD lung tissue and fibroblasts as well (Ng-Blichfeldt *et al.*, 2019). Pharmacological activation of these pathways has also led to promising results in *in vivo* models. For instance, activation of the Wnt/β-catenin signaling pathway with lithium chloride attenuated emphysemic phenotypes by improving lung function and decreasing airspace enlargement in a mouse model (Ng-Blichfeldt *et al.*, 2019). In some rat and mouse emphysema models, activating RA receptors (RARs) with all-trans RA (ATRA) induced alveolar regeneration and improved lung function (Ng-Blichfeldt *et al.*, 2019). ATRA actually proceeded into clinical trials but failed to improve lung function after treatment (Ng-Blichfeldt *et al.*, 2019; Sun *et al.*, 2018). Another trial with palovarotene, a selective agonist of RAR-γ, also failed to show significant efficacy by not improving lung function (Ng-Blichfeldt *et al.*, 2019; Sun *et al.*, 2018).

Although these trials along with the MSC trials have not yet procured promising treatments, there is still potential for regenerative strategies to be used therapeutically. The regenerative signaling pathways already mentioned (and some not mentioned here) can be furthered studied. More research needs to be done to thoroughly characterize these pathways to identify more promising targets and better understand how they function in lung regeneration.

Using 3D human-based disease models for pharmacological studies

Animal models are heavily utilized to study COPD induced by CS exposure including mice, guinea pigs, rats, and dogs (Ghorani et al., 2017). These models along with immortalized human lung cell lines have contributed greatly to COPD research, but there are caveats to using them. For example, the lung anatomy and some COPD disease phenotypes vary in mouse and rat models when compared to human (Zscheppang et al., 2018). Treatments that appear to be effective in rodents may not necessarily be effective in humans as a result. Hence, the use of human-based disease models can be used to more effectively understand the cellular mechanisms underlying COPD (including the mechanisms of relevant targets found through model organisms) and evaluate the efficacy of treatments. A variety of these models exist to study the airway epithelium. Most models are composed of primary cells from donor lungs that are grown under submerged conditions or at air-liquid interface on Transwell inserts where they can differentiate into secretory and ciliated cells (Hiemstra et al., 2019; Zscheppang *et al.*, 2018).

Recently, more complex 3D cell culture models have been developed. Unlike previous models, they allow for more representative human disease modeling by mimicking the structure of the lung and exposing cells to physiological mechanical cues (Hiemstra *et al.*, 2019; Zscheppang *et al.*, 2018). These models include organoids, which are self-assembling structures that are generally derived from stem/progenitor cells and embedded into a 3D matrix. Organoids can be generated from mouse or human cells, and they can be formed by variety of cell types including alveolar cells, airway secretory cells, and airway basal cells (Barkauskas et al., 2017). Considering that they are derived from stem cells, organoids are useful in studying lung formation and repair and epithelial function. These mechanisms are dysfunctional in COPD, so in a disease context, organoids can aid in identifying and understanding targets that underlie these

mechanisms. In addition, organoids can be useful in identifying potential therapeutics. For example, screens have been developed to find compounds that regulate basal cell differentiation and affect the ratio of ciliated and secretory cells, which is disrupted in COPD (Barkauskas *et al.*, 2017). While these screens can be done with ALI cultures, organoid screens are faster, and many more samples can be evaluated (Barkauskas *et al.*, 2017). Overall, organoids have the potential to identify new treatments and identify new disease mechanisms.

In a similar vein, precision cut lung slices (PCLS), is another 3D model that mimics the complexity of the lung. They are lung tissue slices that encompass more of the lung's complexity by containing all the cell types and the ECM composition in a particular area (Alsafadi et al., 2020; Liu et al., 2019). In the context of COPD, PCLS have been used to study the effects of tobacco smoke exposure on different targets, including the previously mentioned study by Zuo *et al.* (Zuo *et al.*, 2018). Studying PCLS from diseased patients also provides useful information on disease and therapeutic mechanisms. For example, Frizzled-4 (FZD4), a WNT receptor, was downregulated in COPD PCLS (Skronska-Wasek et al., 2017). Pharmacological activation of FZD4 with valproic acid induced Wnt/β-catenin signaling and elastogenic components like insulin-like growth factor 1 (IGF1) in COPD PCLS, making it a potential therapeutic target (Skronska-Wasek *et al.*, 2017). In addition, PCLS have also been helpful in elucidating mechanisms for current treatments. In a study by Koziol-White *et al*., the researchers demonstrated that the combined use of a glucocorticoid (budesonide) and a β_2-agonist (formoterol) additively promoted bronchodilation as opposed to either drug alone in PCLS (Koziol-White et al., 2020). Other experiments in both human PCLS and airway smooth muscle cells revealed that budesonide increases cAMP production, which further promotes bronchodilation by adding to the cAMP already released via β_2-agonist treatment (Koziol-White *et al.*, 2020). Overall, these studies are just a few examples of

how PCLS can be used to study disease mechanisms and evaluate therapeutic responses, which will be beneficial for future therapeutic development.

Another model with similar characteristics to organoids and PCLS is lung-on-a-chip. Lung-on-a-chip is a microfluidic device composed of microchannels lined with human cells that are exposed to a continuous flow of nutrients and growth factors. Many different types of models have been developed by different groups based on diseases and research areas (Shrestha et al., 2020). Some lung-on-a-chip models for asthma and COPD were developed in a study by Benam *et al*. (Benam et al., 2016). They interestingly demonstrated that their model could be used as a tool to evaluate therapeutic responses (Benam *et al.*, 2016). An experimental anti-inflammatory bromodomain-containing protein 4 (BRD4) inhibitor suppressed neutrophil adhesion to inflamed cells on the chip. Interestingly, when the same drug was tested on 2D Transwell cultures, the efficacy of the BRD4 inhibitor was reduced (Benam *et al.*, 2016). This result suggests that the inhibitor depended on the existence of flow in the model, demonstrating that the microfluidic aspect of the model was also useful in evaluating the mechanism of action for this drug (Benam *et al.*, 2016). The results from this study and others exhibit the potential for lung-on-a-chip as a tool for drug studies in the future (Shrestha *et al.*, 2020). Like organoids and PCLS, lung-on-a-chip simulates lung tissue more closely, making it valuable in evaluating therapeutic responses and predicting whether treatments will be clinically relevant.

Using model organisms as discovery tools

As mentioned previously, animal models have been useful in understanding disease progression and effects of different treatments. While these models are useful in understanding the progression of disease and the effects of specific therapeutic targets, these animal models are rarely used to identify disease-relevant (and potentially novel)

pathways in lung disease. In the few cases where they are, the processes to do so appear complex. Hence, the use of simpler model organisms is one way to bypass this complexity and perform genetic screens more easily and/or at a larger scale (**Figure 1.3**). Studies with *Drosophila melanogaster* and *Caenorhabditis elegans* have procured pathways or recapitulated known pathways that are relevant to COPD (Green et al., 2009; Prange et al., 2018). In *Drosophila*, RNA sequencing of trachea tissue from untreated and CS-exposed larvae revealed that gene expression was altered for 143 genes (Prange *et al.*, 2018). Interestingly, some of these genes function in Nrf2, TGF-β, and JAK/STAT signaling pathways. These pathways have already been identified as relevant to COPD disease progression, making *Drosophila* another option to study these pathways in terms of CS exposure (Prange *et al.*, 2018). As for *C. elegans*, the impact of CS exposure on genes that regulate innate immunity was investigated through microarray analysis. One of the genes identified, *lbp-7*, encodes for a lipid binding protein (Green *et al.*, 2009). Interestingly, mRNA levels for the human orthologue of *lbp-7*, Fatty Acid Binding Protein 5 (FABP-5), were lower in COPD patient cells compared to cells from non-diseased smokers (Green *et al.*, 2009).

In lieu of using model organisms as discovery tools for COPD, I contributed to a project that involved using *Dictyostelium discoideum*, a social amoeba, to identify disease-relevant pathways in the first portion of my thesis (Kliment *et al.*, 2021). In a genetic selection for suppressors against CS-induced insults, a variety of genes came out as protective against CS (Kliment *et al.*, 2021). This list of suppressors included cytoskeletal, metabolic, protein folding, and translational proteins (Kliment *et al.*, 2021). We were interested in further studying one of the proteins, adenine nucleotide translocase (ANT), because of its robust protection against CS in *Dictyostelium*. ANT is a mitochondrial protein in the inner membrane that is responsible for transporting ATP/ADP in and out of the mitochondria (Liu and Chen, 2013). Interestingly, ANT

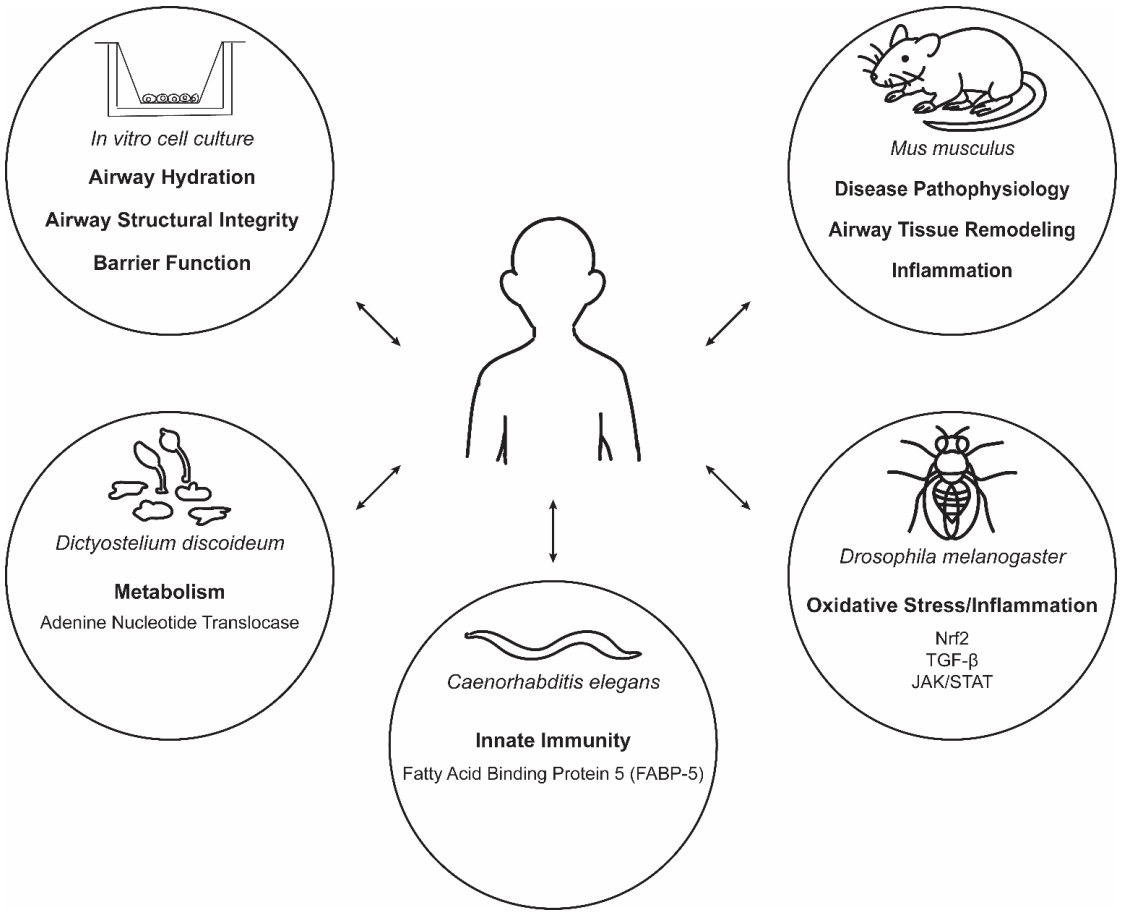

Figure 1.3. Various model organisms can be utilized to identify new and relevant biology in COPD. Mice have been heavily used to study COPD and understand disease progression, but the processes that come with identifying new essential disease biology are more complex in both human and mouse. Interestingly, there is emerging research on finding additional disease-relevant biology with simpler model organisms. New pathways affected by cigarette smoke have been identified in in vitro cell culture models, *C. elegans* (23), *Drosophila* (47), and social amoeba *Dictyostelium discoideum* (32). By utilizing these simpler models, there is the potential to recapitulate major findings or discover novel research on COPD, which can then be further studied in complex systems such as human and mouse.

appears to be a novel target for COPD outside of inflammation. Hence, we conducted further studies to understand how it is protective against CS and assess its relevance to disease onset and progression. We proceeded to study ANT in human disease models in the context of previously mentioned research areas that may underlie COPD (*i.e.,* mitochondria and airway hydration).

As a follow-up to the first portion of my thesis work, the second portion focuses on ANT in the less obvious context of cell mechanics and cytoskeletal systems. Our lab previously established that defects in cytoskeletal systems in *Dictyostelium* are bypassed through the overexpression of ANT (Kliment *et al.*, 2021). From our COPD studies, we discovered that ANT affects ATP production. This result suggests that cytoskeletal function affects ATP production in a more complex feedback system contrary to the traditional view of ATP flowing into cytoskeletal remodeling. Since CS also affected cells by altering cell structure and affects ATP production, it was of interest for us to observe whether ANT can alter cellular structure by increasing ATP production (Kliment *et al.*, 2021; Nishida *et al.*, 2017). Based on these findings, we can further elucidate how ANT is protective against CS, potentially through changes in cellular structure.

Note: Text and figures have been adapted from (Nguyen et al., 2021).

Chapter 2: Materials and Methods

Cell strains and culture

Human cell culture

Human bronchial epithelial cells (HBE), immortalized by Cdk4 and hTERT, were a gift from John Minna (University of Texas Southwestern Medical Center, Dallas, Texas). HBE cells were generally grown in keratinocyte serum-free media (ThermoFisher). When these cells reached 70-80% confluent, they were split after being trypsinized with 0.05% trypsin and treated with trypsin neutralizing solution.

Primary normal human bronchial epithelial cells (NHBE) were obtained from Lonza and MatTek. Vials of cells were thawed and grown on flasks coated with Type I collagen (50 µg/ml in 0.02N acetic acid). After cells reached 80-90% confluency, they were split after trypsinization with 0.05% trypsin and neutralization with trypsin neutralizing solution. Cells were seeded on PET inserts coated with Type I collagen at a density of 90,000 cells per 12-well insert (0.4-µm pore, 1.12 cm^2 area, Corning Costar) or 30,000 cells per 24-well insert (0.4-µm pore, 0.33 cm^2 area, Corning Costar) with both apical and basal media. Once a confluent monolayer was formed, apical media was removed, and cells were grown at air liquid interface (ALI) for three-six weeks until they differentiated into an airway epithelium.

NHBE cells from Lonza and MatTek were initially grown in BEGM media (Lonza) with recommended supplements (bovine pituitary extract, insulin, hydrocortisone, epinephrine, transferrin, recombinant human epidermal growth factor, retinoic acid, triiodothyronine (T3), and gentamicin sulfate amphotericin-B) with additional bovine pituitary extract (12.6 µg/mL, AthenaES), bovine serum albumin (BSA) (final concentration of 1.5 µg/mL, Sigma-Aldrich), retinoic acid (final concentration of 0.1 µM) and epidermal growth factor (final concentration of 25 ng/mL). When NHBE cells were grown at ALI, BEGM media (Lonza) and DMEM media were combined with

recommended Lonza supplements (1 supplement pack per 500 mL of media) with additional bovine pituitary extract (12.6 µg/mL, Lonza and AthenaES), BSA (final concentration of 1.5 µg/mL, Sigma-Aldrich), and retinoic acid (final concentration of 0.1 µM).

Dictyostelium cell culture

A list of transformed strains used is provided in **Table 1**. Vegetative *D. discoideum* cells were routinely grown in Hans' Enriched HL-5 (1.5x HL-5 medium supplemented with ForMedium (FM, 8% final concentration), penicillin (60 U/mL), and streptomycin sulfate (60 mg/mL)). Cells were grown at 22°C on polystyrene Petri dishes and passaged by simple pipetting before cells reached the stationary phase (between $2x10^6$ and $6x10^6$ cells/mL). Cells grown in suspension were placed in Erlenmeyer flasks at 180 rpm at 22°C.

Table 1. List of transformed *Dictyostelium* strains used

Background Strain	Plasmids transformed
KAx3	pDM181
cortI	pDM181
cortI	pDM181:*mCherry-cortI*
cortI	pLD1A15SN:*ancA*

Mutant cell line generation

Adenovirus gene expression in human bronchial epithelial cells

Adenovirus constructs were developed for gene delivery of control eGFP, ANT1-GFP (Ad-h-*SLC25A4*/eGFP, GenBank BC008664.1), and ANT2-GFP (Ad-h-*SLC25A5*/eGFP, GenBank BC056160.1) from Vector Biolabs (Malvern, PA) in NHBE and HBE cells. Cells were infected with an MOI of 40-80. Protein expression and localization were confirmed. Adenoviral infection efficiency was ~85–95% with confirmed

expression of ANT-GFP isoforms. Adenoviral infected cells were used for experiments 48 h after initial virus exposure.

Dictyostelium mutant cell line generation

The plasmids for the untagged, GFP-tagged, or mCherry-tagged fusions of *myosin-II heavy chain (mhcA)*, *cortexillin-I* (*ctxA*), *racE*, and *ancA* have been described previously (Effler et al., 2006; Kee et al., 2012; Kliment *et al.*, 2021; Lee et al., 2010; Ren *et al.*, 2014). *Dictyostelium* cells were transform with 1 µg of expression plasmids using a Genepulser-II electroporator (Bio-Rad, Hercules, CA). Transformed cells were grown in enriched Hans' HL-5 media for 24-48 hr at 22°C before being grown in Hans' enriched HL-5 with G418 (typically 10-15 µg/mL but determined using kill curves and/or optimization of transformation efficiency with the empty plasmid). Media with drug was changed every 2-3 days until clones were harvested.

In vitro cigarette smoke exposure

Cigarette smoke exposure comprised of either treatment with cigarette smoke extract (CSE) or gaseous CS through the Vitrocell system. CSE was made by bubbling one research grade cigarette (Type: 3R4F, Tobacco Health Research Institute, University of Kentucky, Lexington, KY) into 25 mL of media over 6 min with a peristaltic pump. This solution was considered 100% CSE, which was then filtered with a 0.22-µm filter. For gaseous CS exposure, NHBE grown on inserts at ALI were inserted into chambers in the Vitrocell system as demonstrated in **Figure 2.1**. Cells were exposed to air or two cigarettes smoked over 16 min using an International Organization for Standardization protocol (McElvaney et al., 1989).

Metabolic studies

MitoSOX studies

Mitochondrial reactive oxygen species production was assessed using MitoSOX Red (ThermoFisher) staining in HBE cells treated with adenovirus and CSE. Cells were

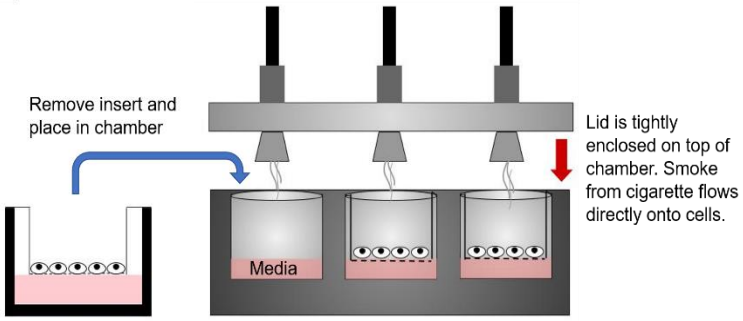

Figure 2.1. Schematic of cigarette smoke exposure chamber of Vitrocell smoking machine. Transwell inserts are kept humidified and at 37°C through the flow of warmed water through the chamber. Smoke is delivered through the funnel positioned directly above the cells at a constant flow rate.

washed once with PBS and incubated with MitoSOX for 10 min at 37°C, 5% CO_2. Cells were washed three times with PBS and placed in L-15 Leibovitz medium for imaging using the High Content Imager. For cell analysis, fluorescence intensity of mitochondria was assessed with exclusion of the nucleus. For cell analysis, MetaXpress software (Molecular Devices) was used to separate cells infected with adenovirus constructs from uninfected cells. The average fluorescence intensities of MitoSOX staining in mitochondria were determined with exclusion of the nucleus. Approximately 300–400 cells were analyzed per well for a total of 700–1500 cells per group. Across all replicates, 2800–4500 cells per group were evaluated.

ATP measurements

HBE intracellular ATP concentrations were measured after cells were seeded onto 6-well plates and infected with adenoviral ANT1, ANT2, and GFP control for 48 hr.

The cells were then treated with media alone or 20% CSE for 4 hr. Cell lysates were collected with lysis buffer and 300 μM of ecto-ATPase inhibitor ARL 67156 (Sigma), flash-frozen in liquid nitrogen, thawed on ice, and boiled for 5 min. The concentration of each sample was assessed via a luciferin-luciferase bioluminescence ATP Determination Kit (ThermoFisher). Luminescence was detected in a microplate reader (FLUOstar Omega, BMG Labtech) and integrated over 10 s. Concentrations were determined using a standard curve with a linear range between 0.5 and 1000 nM ATP. The ATP concentration in mM per HBE cell was calculated by considering the cellular volume of and the amount of ATP in a single HBE cell as demonstrated in the following equation: Amount of ATP per cell = (Concentration of ATP per cell) (Volume of cell). Spherical cell volume was determined after measuring the diameter of trypsinized HBE cells on an epifluorescence microscope (Olympus). The amount of ATP for one cell was derived from the amount of protein in one cell found via Bradford assay (BioRad).

For *Dictyostelium* cells, cytoskeletal mutants, their respective rescue lines, and ANT overexpressed cell-lines were prepared beforehand. Their intracellular ATP was measured via luciferin-luciferase as described above. *Dictyostelium* spherical cell volume was determined after measuring the diameter of settling cells after resuspension on an epifluorescence microscope.

Seahorse XF mito stress assay

The following protocol was adapted from (Lay et al., 2016). The Seahorse XF mito stress assay (X96 Flux Analyzer, Agilent) was used to assess metabolic activity for *Dictyostelium* cytoskeletal mutants. Cells were resuspended in SIH media (FM media with final concentrations of 20mM sodium pyruvate and 5mM malic acid, pH to 7.4) in 96-well Seahorse assay plate coated with Matrigel (Agilent). Oxygen consumption rate (OCR) was measured through the Seahorse Flux Analyzer according to the

manufacturer's protocol (Agilent). After 3 basal measurements, various drugs were injected into wells and mixed before subsequent OCR measurements. Oligomycin (20 μM, ATP synthase inhibitor) was injected, followed by FCCP (10 μM, mitochondrial uncoupler), Rotenone (30 μM, ETC complex I inhibitor), and then Antimycin A (30 μM, ETC complex III inhibitor). The data output results in various metabolic outputs such as basal respiration, ATP production, maximal respiration, spare respiratory capacity, proton leak, and non-mitochondrial respiration.

Ciliary function studies

Airway surface liquid (ASL) height

ASL height was measured by adding 10 kD-Texas Red-dextran (ThermoFisher, diluted in PBS) to NHBE or HBE cells grown at air liquid interface (17.5 μL per 12-well insert and 6.7 μL per 24-well insert). The apical surface was washed with PBS about 16 hr prior to the addition of Texas Red-dextran. After 4 hr of incubation with Texas Red-dextran, cells were imaged. Right before imaging, Fluorinert (100 μL per 12-well insert and 30 μL per 24-well insert, Sigma) was added to the apical surface to prevent evaporation. Inserts were imaged on a Zeiss 780 confocal microscope equipped with a heat and CO_2 controlled stage and 40x water objective. ASL was imaged by acquiring 3x3 or 4x4 tiled z-stacks, and each z-stack image was captured at a step size of 0.46 μm. For experiments with ANT inhibitors, carboxyatractyloside (CATR, 20 μM, Sigma) and bongkrekic acid, (BKA, 4 μM, Sigma) in PBS were added to the Texas Red dextran dye and applied to the apical surface of ALI cultures 4 hr prior to ASL assessment. For apyrase treatment, 10 units of apyrase (Sigma) was added with Texas Red-dextran as described above 4 hr prior to ASL assessment.

Thickness across the sample was computed using a custom script, written in Matlab (Mathworks, Natick, MA). Briefly, for each value *x* in the three-dimensional images, Im(*x, y, z*), the resultant (*y, z*) slice was segmented using adaptive thresholding (Matlab command: imbinarize), followed by operations to fill holes (imfill), morphological opening (imopen) and filtering of small regions (bwareaopen). The threshold level was adjusted after preprocessing the complete image and the process repeated. For each y in this binary image, the number of segmented pixels was counted, giving a measure of the thickness in the (x, y) location; see Supplementary Information 1. This gave a histogram of depths over the image. An average depth was computed for all pixels in which a non-zero depth was detected (to avoid edge effects). The process was repeated by fixing y and working with the (x, z) slice. The differences between the averages were typically less than 1–2%. Thickness in pixels was converted to μm using a slice thickness of 0.46 μm, the step size used to collect the z-stack.

Ciliary beat frequency

NHBE cells were infected with adenovirus 48 hr before ciliary beat frequency was assessed. Inserts at ALI were placed in a 12-well Falcon plate and supplemented with L-15 Leibovitz medium, and they were then imaged 2 min later. Videos were taken on a Leica spinning disk confocal with a 40x water objective. About 3-5 videos were taken for each insert from the top down at 160 frames/s over 4 s. Each insert was treated with either air or CS through the Vitrocell system before being imaged again. After this second imaging session, cells rested for 4 hr afterwards at 37°C and 5% CO_2 before being imaged for a third time.

Ciliary beat frequency (CBF) was measured using a custom Matlab script. Individual images from a video consisting of *N* frames were used to create a three-dimensional matrix Im*k* (*x, y*), where (*x, y*) denotes location in the image of each pixel,

and $k \in 1, \ldots, n$ is the frame number. For each (x, y), the corresponding sequence of intensities was first normalized:

$$p_{i,j}(k) = \frac{\mathrm{Im}_k(x,y) - \min_k \mathrm{Im}_k(x,y)}{\max_k \mathrm{Im}_k(x,y) - \min_k \mathrm{Im}_k(x,y)}$$

so that $0 \le p_{i,j}(k) \le 1$ and filtered by removing the mean value:

$$\tilde{p}_{i,j}(k) = p_{i,j}(k) - \frac{1}{N}\sum_{k=1}^{N} p_{i,j}(k).$$

The Fast-Fourier transform (FFT) of $\tilde{p}_{i,j}(k)$ was obtained using the MATLAB command fft:

$$q_{i,j}(n) = \sum_{k=1}^{n} p_{i,j}(k) e^{-2\pi i n k/N}, \qquad n = 0, \ldots, N-1.$$

and the corresponding single-sided power spectrum was computed (where N is even):

$$\tilde{q}_{i,j}(n) = \begin{cases} |q_{i,j}(0)|, & n = 0 \\ 2|q_{i,j}(n)|, & n = 1, \ldots, N/2 \end{cases}$$

This gives a power spectrum for each pixel.

To determine the frequency of beating, we carried out two approaches. In the first, we found the frequency with highest power density for each of the pixels. We then used a threshold (set at 0.125 A.U.) to determine whether there was any detectable power in that pixel or not. The frequency with highest power was determined, and this data aggregated over all pixels meeting this threshold. The data between 2 and 20 Hz of the corresponding histogram was then normalized and fit by a single Gaussian, $\alpha \exp^{-((f-\mu)/\sigma)^2}$ where f is the frequency, using the command fit. The value of μ was used as a measure of beating frequency.

In the second method, we aggregated the power spectra from all pixels (with no thresholding): $\bar{q}(n) = \sum_{i,j} \tilde{q}_{i,j}(n)$ and fit the data between 2 and 20 Hz to a Gaussian mixture model using three modes. This resultant μ value with the greatest contribution to

the mixture model was used. Both methods provided similar estimates, so the data we reported in our publication used Method 1 frequencies.

Immunofluorescence imaging

For paraffin-embedded human lung tissue, samples were adhered to slides for 60 min at 60°C on a slide warmer and then deparaffinized with xylene and ethanol. Samples were then placed in sodium citrate at 95°C for 20 min for antigen retrieval. For HBE grown on slides or on inserts at ALI, cells were fixed in ice-cold 4% paraformaldehyde for 10 min. Prepared human lung tissue or cells was processed as described below.

Samples were washed with 1x PBS three times and then blocked in 1X PBS + 0.05% Triton X-100 + 0.5% BSA for 45 min at room temperature. This was followed with 3 washes in 1X PBST (1X PBS + 0.05% Triton X-100). Primary antibody was incubated on sections in PBST overnight at 4°C. Samples were washed with PBST 5 times on the next day. They were then incubated with secondary antibody in PBST for 60 min at room temperature, away from light, and then washed with PBST 5 times. For inserts at ALI, the transmembrane was cut out and placed on glass slides. Sections were mounted in Prolong Diamond Antifade Mounting Agent (Molecular Probes, ThermoFisher) and allowed to cure for at least 24 hr at room temperature in the dark. Images were routinely taken on Zeiss confocal microscopes at 40x or 63x with excitation lasers at 488 for GFP, 561 for mCherry, and 633 for far-red fluorescent proteins. Sections were stained with the following primary antibodies: ANT1 (Abcam #ab102032 rabbit polyclonal, 1:100), pan ANT (anti-ANT1/2/3 Abcam, #ab110322, mouse monoclonal 1:100), ANT2 (5H7, from S. Claypool (Jones et al., 1992), 1:100), ANT2 (Abcam, #ab118076, mouse monoclonal, 1:100), ANT2 (Abcam, #ab222843, 1:100), ANT2/3 (Abcam, #ab230545, 1:100), and goat anti-mouse, anti-rabbit or anti-chicken Alexa 488, 555 and 647 (Molecular Probes).

Dictyostelium cell viability

Cells were seeded in 10 mL of Hans' Enriched HL-5 medium in 150 mL Erlenmeyer flasks at a starting concentration of $1x10^5$ cells/mL. They were shaken in 22°C incubator at 180 rpm, and the cell concentration was measured and recorded roughly every 24 hr using a hemocytometer. When cells reached the later point of exponential growth phase (about $5\text{-}6x10^6$ cells/mL), cultures were split down to a concentration of 0.5 - 1 x 10^5 cells/mL. Cell density continued to be measured roughly every 24 hr. Data was normally acquired from second and third cycles of suspension culture. Relative growth rates were determined by plotting cell densities versus time. The resulting exponential phase curves were fitted to single exponential equations using KaleidaGraph (Synergy Software). Growth rate (*k*) was determined for each growth curve through the exponential growth equation:

$$n(t) = n_0 e^{kt}$$

where n(t) = population at time t, n_0 = initial population concentration, and *k* = relative growth rate.

Western analysis

Western analysis was done with lysates from *Dictyostelium*, human airway epithelial cells, and yeast *S. cerevisiae*. Protein concentration was determined by Bradford Assay (Pierce). Human airway lysates were obtained using RIPA buffer with protease inhibitor cocktails I, II, and III (Sigma), RNase, and 150 nM aprotinin. *Dictyostelium* lysates were obtained after flash freezing samples in liquid nitrogen. Yeast protein lysates were obtained from yeast expressing human ANT1-4 (Δ*aac[EV],* Δ*aac[ANT1],* Δ*aac[ANT2],* Δ*aac[ANT3],* Δ*aac[ANT4],* OD_{600}=3 per group) via alkaline lysis with NaOH/β-mercaptoethanol and trichloroacetic acid. Samples were run on 10-15% acrylamide gels and transferred onto nitrocellulose membranes. Blots were

incubated with primary antibodies overnight at 4°C and then imaged on the Li-Cor Odyssey CLx Blot Imager using Li-Cor fluorescent secondary antibodies. The following primary antibodies were used: human ANT1 (1:500, ab1F3H11 from Steven Claypool, mouse), ANT2 (1:500, ab5H7 from Steven Claypool (Jones *et al.*, 1992), mouse), ANT2 (1:500, ab5695 from Steven Claypool, rabbit), ANT1 (1:500, Abcam, #102032, rabbit), pan ANT (1:500, anti-ANT1/2/3 Abcam, #ab110322, mouse), ANT2 (1:500, Abcam, #ab118076, mouse), ANT2 (1:500 Abcam, #ab222843, rabbit), and ANT2/3 (1:500, Abcam, #ab230545, rabbit).

Statistics

Normally distributed data was analyzed with an ANOVA followed by a Fisher's LSD post-test. Kruskal-Wallis and Mann-Whitney were used for nonparametric data sets. Statistical analysis was performed and graphed using KaleidaGraph (Synergy Software) or Graphpad Prism.

Note: Some text has been adapted from (Kliment *et al.*, 2021).

Chapter 3: Adenine Nucleotide Translocase as a Protector Against Cigarette Smoke Through Regulation of Metabolism, Airway Hydration, and Ciliary Function

As previously mentioned, our lab previously identified adenine nucleotide translocase (ANT) as protective against cigarette smoke (CS) by utilizing *Dictyostelium discoideum* as a discovery tool. Using *Dictyostelium*, we created ~35,000 transformants with a cDNA library and grew them in a cigarette smoke extract (CSE) made from media bubbled with CS, one of the main causes of COPD. We selected for transformants that were protected from CS-induced growth defects and isolated their genes. ANT was a gene that offered complete protection of cell viability against CS (Kliment *et al.*, 2021). When studies were transferred into immortalized human bronchial epithelial cells (HBE), we found that ANT also protected against CS by increasing cell viability. With this information, we were interested in understanding the protective mechanisms of ANT against CS. By understanding the core cellular processes of ANT in human or mouse models, we hope to harness their protective properties to treat COPD (*i.e.* screen for pharmacological agents that will promote target activation and induce protective phenotypes). Overall, this project was a large collaborative effort between many talented scientists. Below, I specifically describe my contributions to this study.

ANT regulates metabolic activity by affecting oxidative stress

As a transporter of ATP/ADP in the mitochondria, we were interested in examining whether ANT regulated mitochondrial activity in the context of CS. Mitochondrial function, as mentioned before, is disrupted after CS exposure. Morphology and metabolism are affected negatively, and mitochondria are also a source of endogenous reactive oxygen species (ROS) when under stress. ROS is considered a significant drive in COPD onset, and interestingly, there is evidence that ANT can

change levels of ROS (Kretova et al., 2014). Thus, we proceeded to examine whether ANT could protect against CS-induced ROS.

MitoSOX Red was used as a marker for ROS in HBE cells. Cells were exposed to either 0% or 20% CSE for 1, 4, or 24 hours and imaged on a high content imager (**Figure 3.1**). We observed that CSE exposure did not significantly affect the levels of MitoSOX. Nonetheless, after 1 hour, ANT1 overexpression decreased MitoSOX expression slightly. Both ANT1 and ANT2 overexpression increase MitoSOX expression after 4 and 24 hours of CSE exposure. Something to note is that each experimental group was heavily sampled through the high content imager, which results in slight changes producing a statistically significant difference. Whether these slight changes are biologically relevant is unknown, but the increase in MitoSOX from ANT1 and ANT2 overexpression may coincide with an increase in electron transport chain flux. This increase in flux is reflected by an increase in cellular respiration, which had been demonstrated in our other metabolic experiments (Kliment *et al.*, 2021).

Intracellular ATP levels of HBE after CS treatment

Other aspects of mitochondrial function in the context of CS that we examined were metabolic activity and ATP production. We demonstrated that ANT overexpression increased ATP production in HBE after exposure to CS via changes in oxygen consumption rate (Kliment *et al.*, 2021). Hence, we proceeded to validate whether this change in ATP production would reflect in changes in the amount of intracellular ATP. Intracellular ATP concentrations can be indicators of cell viability and energetic state, and there is evidence that CS can affect the concentration of ATP (van der Toorn et al., 2007). We measured the amount of steady-state ATP in HBE cells using a luciferin-luciferase assay and found the concentration to be around 8 mM of ATP per cell. ATP concentrations were also measured after exposure to 20% CSE, and interestingly we did

not see a difference from control cells and in cells overexpressing ANT1 or ANT2 (**Figure 3.2**). This result could indicate that while steady-state concentrations of ATP do not change in the cell, ATP flux could still increase or decrease, and this coincides with the cell using more or less energy overall.

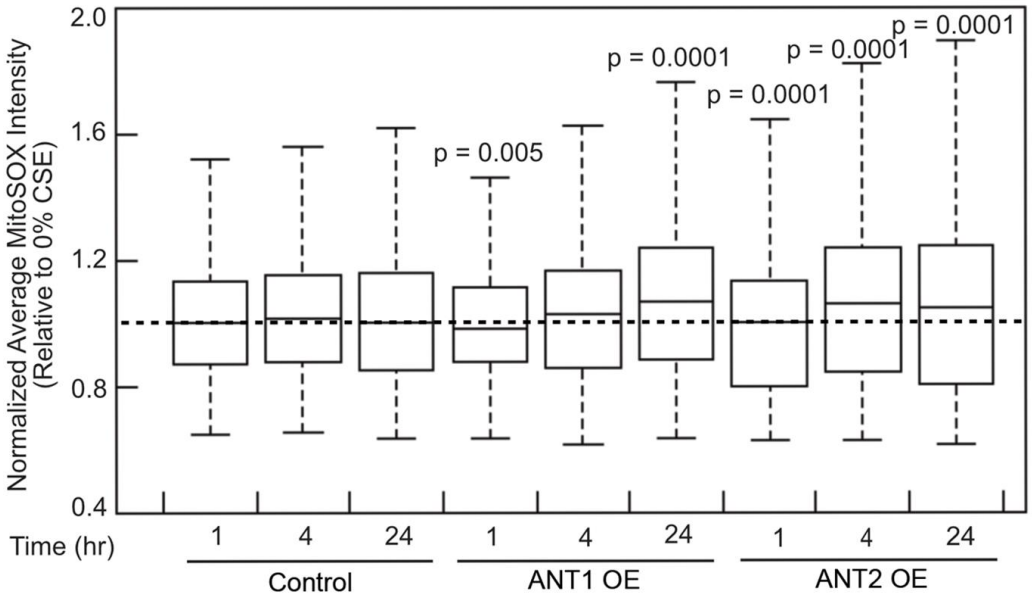

Figure 3.1. ANT modulates mitochondrial reactive oxygen species. Boxplot showing mitochondrial superoxide production (MitoSox) in HBE after CSE with ANT overexpression. Horizontal dotted line represents the median for the 1 hr control group. Boxplots show the median with the box delineating the 1st and 3rd quartiles. The whiskers represent 1.5*IQR (interquartile range). Statistics performed by Kruskal-Wallis and two-tailed Mann-Whitney U tests. P-values represent differences from Control at each respective time point. n = 2800-4500 cells per group.

ANT enhances airway hydration and ciliary function

As stated previously, the airway epithelium acts as a barrier to toxins and particulates and removes them from the airway. Airway hydration and normal ciliary function are important components to the epithelium's barrier function and are both negatively affected by CS exposure. In addition, ATP plays an important role in maintaining normal ciliary function via providing energy for ciliary beating (Lazarowski et al., 2004). Extracellular ATP is also responsible for signaling pathways that activate the

cystic fibrosis transmembrane conductance regulator (CFTR) and block the epithelial sodium channel (eNaC). This blockage of eNaC and activation of CFTR results in airway hydration by the release of chloride ions and water (Huang et al., 2001). The importance of ATP in ciliary beating and airway hydration propelled us to examine whether ANT could regulate them.

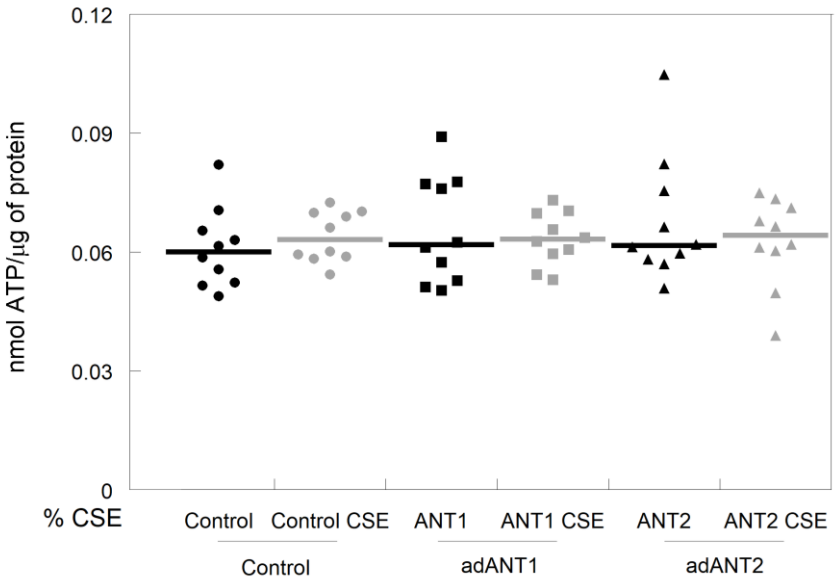

Figure 3.2. Total intracellular ATP does not change after cigarette smoke treatment or with ANT overexpression. Measurements of total intracellular ATP in HBE with ANT1 or ANT2 overexpression ±20% CSE, yielding a total intracellular [ATP] of 8 mM for HBE cells. Median bars shown; n = 10 wells per group from 5 separate experiments.

We proceeded to assess airway hydration and ciliary beating with ANT overexpressed in normal bronchial epithelial cells (NHBE) grown at air liquid interface (ALI). These cells differentiated into an airway epithelium, and we confirmed that they produced beating cilia. We also confirmed both ANT1 and ANT2 expression in these cells after adenoviral infection. To assess airway hydration, the height of the airway surface liquid (ASL, the liquid layer atop the airway epithelium) was measured via confocal microscopy. Interestingly, ANT2 overexpression increased ASL height about 2.3-fold above GFP-control cells and ANT1-overexpressed cells (**Figure 3.3A**). To verify

that ANT activity increased ASL height, we also measured ASL height after treating cells with inhibitors of ANT, carboxyatractyloside (CATR) and bongkrekic acid (BKA). Both inhibitors abrogated the increase in ASL height by ANT2 overexpression (**Figure 3.3A**). In addition, we also used apyrase, an ATP hydrolyzer, and it prevented the increase in ASL height by ANT overexpression as well (**Figure 3.3A**). This result confirmed that the presence of extracellular ATP was required for an increase in ASL height. Overall, ANT2 overexpression increased ASL height via extracellular ATP, suggesting that it regulated airway hydration. We found that ANT2 can actually regulate airway hydration regardless of whether cells had cilia. HBE cells, which do not grow cilia, were grown at ALI and ASL was measured. ANT2 overexpression in HBE caused an upward trend in ASL height, and this increase in height was also inhibited by CATR and BKA (**Figure 3.3B**).

To assess ciliary beating, videos were taken of NHBE treated with air or gaseous CS and ciliary beat frequency (CBF) was measured. There was no significant difference in CBF between air-treated control and ANT2 overexpressed cells (**Figure 3.4**). CS did slow down CBF for control cells, but ANT2 overexpression notably did not alter CBF (**Figure 3.4**). Even after a rest period, CBF continued to persist at baseline in CS-treated cells overexpressing ANT2 while CBF for control did not return to baseline (**Figure 3.4**).

ANT localizes to the plasma membrane of differentiated NHBE

As stated before, the release of extracellular ATP contributes to airway hydration (Schwiebert and Zsembery, 2003). A few transporters have been implicated in shuttling ATP outside of the cell, but the list is not yet exhaustive (Schwiebert and Zsembery, 2003). Because CATR, a membrane-impermeable inhibitor, blocked the increase in ASL height caused by ANT2, we hypothesized that ANT2 may be localizing to the cell surface. If so, ANT2 could be functioning as an extracellular ATP transporter.

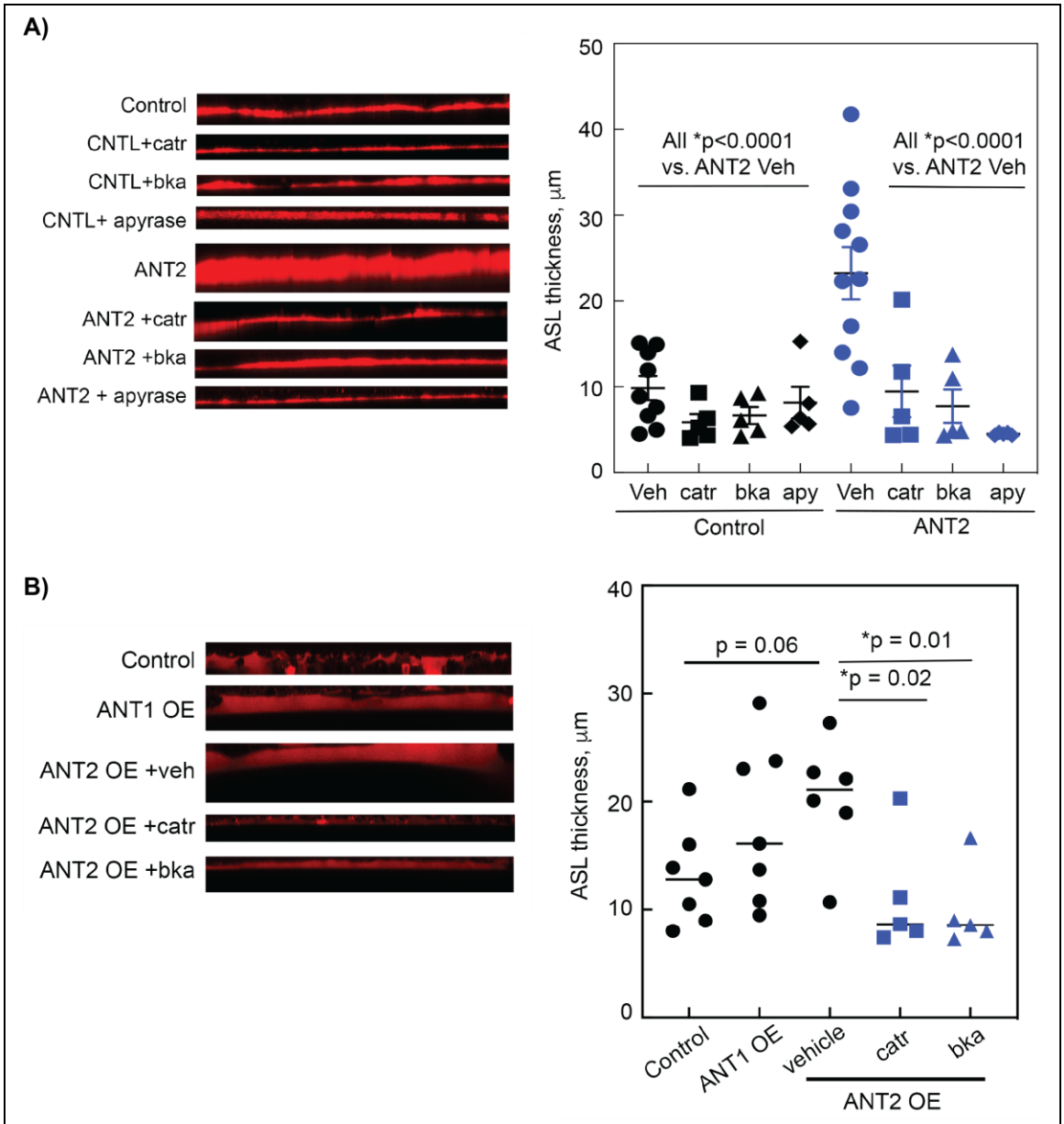

Figure 3.3. Airway surface liquid height increases with ANT2 overexpression. A) X-Z plane confocal images of ASL labeled with Texas Red- dextran were collected and used to measure ASL thickness. Images were also taken of NHBEs treated with ANT inhibitors, carboxyatractyloside (catr, 20 µM) and bongkrekic acid (bka, 4 µM), and an ATP hydrolyzer, apyrase (apy). n=5-11 inserts with *P*-values as presented. **B)** ASL was also measured for HBE cells, which do not have cilia. Representative orthogonal views of ASL height from HBE cells and ASL quantification are presented. n=5-7 inserts with *P*-values as indicated.

We analyzed ANT localization in both human lung tissue and NHBE cells grown at ALI (Kliment *et al.*, 2021). For the NHBE cells, vertical sections of the inserts were cut

and processed for immunofluorescence imaging (IF). Through IF, ANT was visibly near the cell surface and along the cilia (**Figure 3.5A**). ANT signal at the cell surface and/or cilia was quantified and compared to IgG control to confirm that the signal was above background (**Figure 3.5B,C,D**). To confirm that the IF signal was indeed ANT, multiple antibodies were used to probe for ANT. These antibodies were confirmed to bind to ANT through western analysis of lysates from yeast expressing human ANT1-4 (**Figure 3.6**).

The experiments done with human lung tissue offered similar results (Kliment *et al.*, 2021). We also confirmed that ANT co-localizes with mitochondrial markers and ciliary markers and that there was no evidence of fluorescence bleed-through from those markers (Kliment *et al.*, 2021). Overall, our localization studies point to ANT being at the cell surface near the cilia, making it poised to be an extracellular ATP transporter.

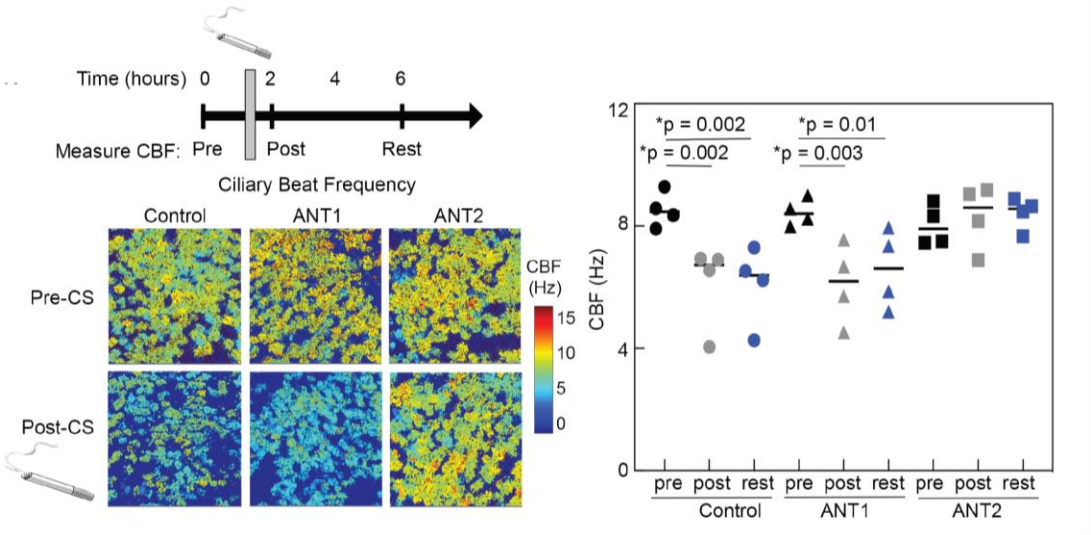

Figure 3.4. Ciliary beat frequency is not altered with ANT2 overexpression after cigarette smoke exposure. Videos were taken of cilia beating on NHBEs before, 30 mins after, and 4 hours after treatment with air or CS. ANT2 overexpression maintains normal CBF after CS treatment while CBF for control and ANT1 cells decreases and remains lower than baseline CBF as demonstrated in the heatmaps and CBF quantifications. CBF stayed at a normal level with ANT2 overexpression even after a 4-hour rest period. n=3 inserts with *P*-values as noted.

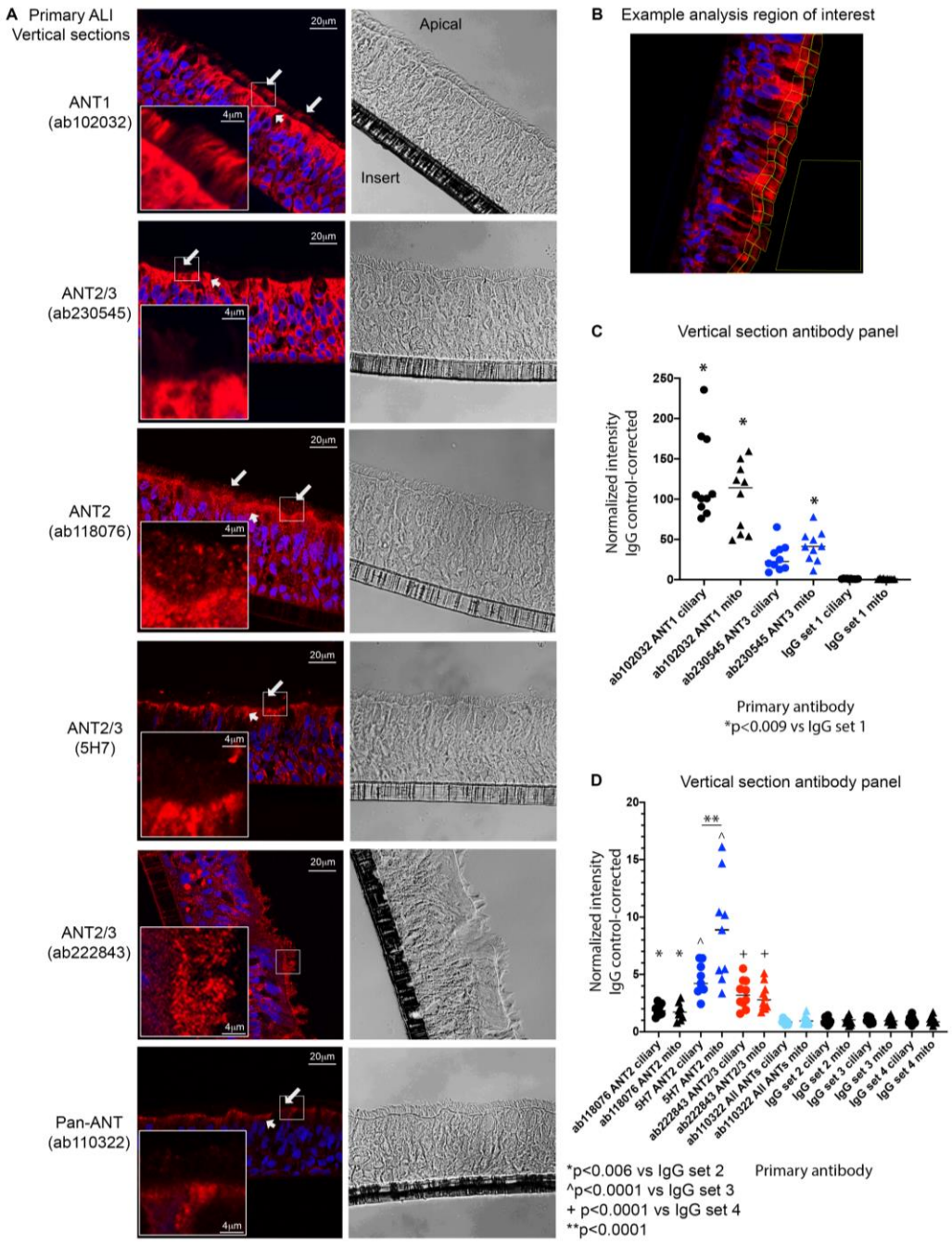

Figure 3.5. ANT localizes at the cell surface and cilia in human bronchial epithelial cells. A) Frozen vertical sections of normal human bronchial epithelial cells grown at air liquid interface were stained with a panel of ANT antibodies (red). Brightfield images are provided to show cilia on the apical surface of the airway epithelium. **B)** For quantification of ANT signal, regions of interest (ROIs) were traced in the cilia, the mitochondrial layer directly below the apical surface, and in the background. **C-D)** ANT signal in the ROIs were background subtracted and normalized to IgG secondary-only controls, demonstrating significant increases in both the cilia and mitochondrial layer. n=cells from 3-5 patients. Results of an ANOVA test with Fisher's LSD. *P*-values are as noted.

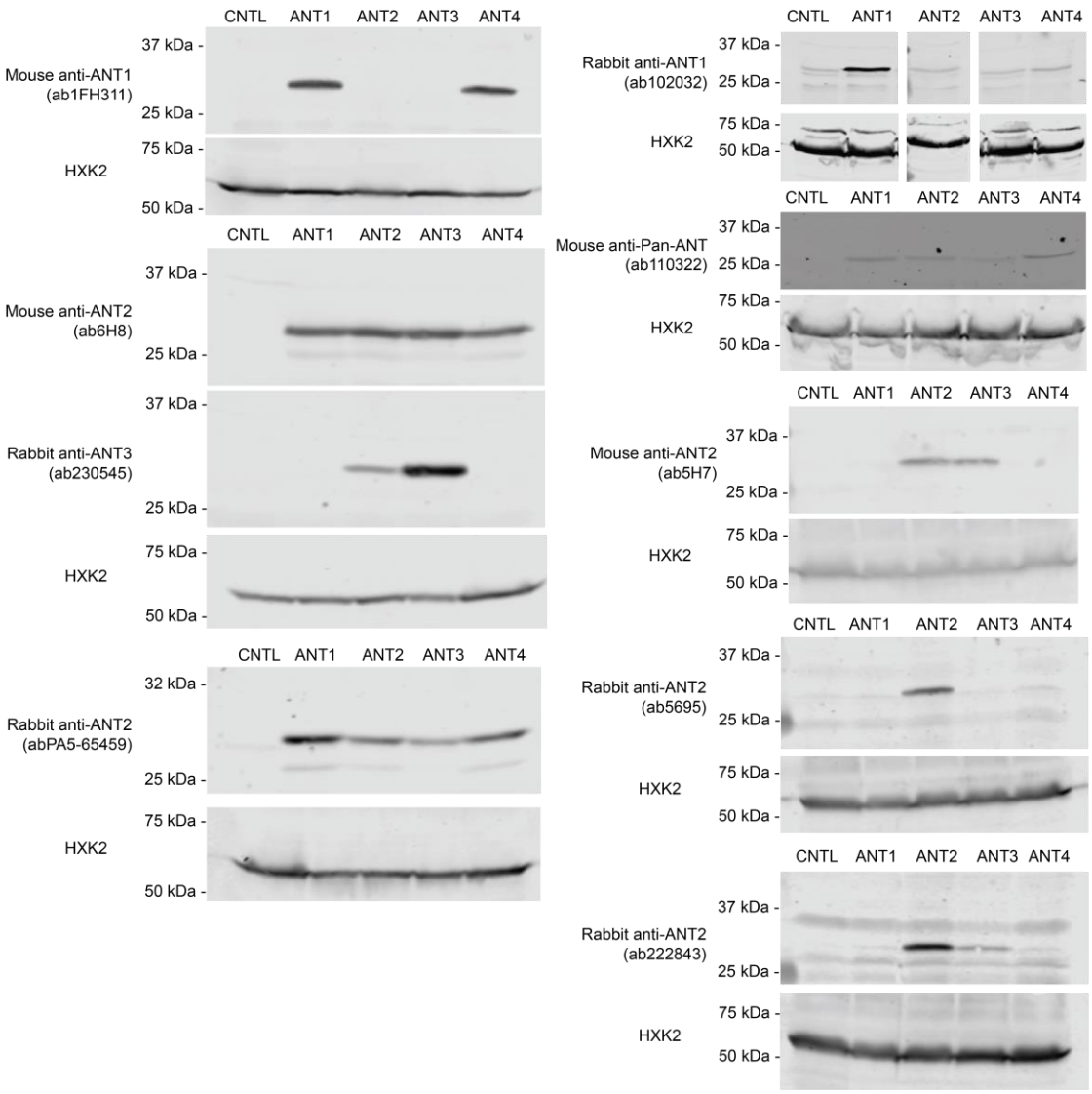

Figure 3.6. Western analysis of ANT antibody specificity. Antibody specificity was determined for rabbit and mouse anti-ANT antibodies utilizing yeast strains with expression of the individual human ANT paralogs, ANT1-4. Hexokinase-2 was used as the loading control.

Note: Text and figures have been adapted from (Kliment *et al.*, 2021).

Chapter 4: Discovering and deciphering the feedback between metabolism and cytoskeletal function

Cell shape change is involved in several processes including cytokinesis, tissue development, wound healing, and immune function. These processes are further implicated in diseases such as pancreatic cancer progression and as mentioned previously, COPD. Maintaining normal airway structural integrity is vital to prevent COPD onset (Aghapour *et al.*, 2018). Our group has found that continual CS affects actin assembly and cell mechanics in NHBE cells (Nishida *et al.*, 2017). This study along with others highlight that cell structure and cytoskeletal function should be topics of interest for COPD therapeutic development.

In the context of ANT, we have several pieces of evidence that point to ANT having interactions with cytoskeletal modulators in *Dictyostelium* (**Figure 4.1**). ANT overexpression acted as a genetic suppressor of two mutants, a null mutant of racE small GTPase and an engineered wild-type strain with integrated assembly-incompetent myosin II phosphomimetic 3xAsp (Ren *et al.*, 2014). Both mutants have defects in cell mechanics and cytokinesis fidelity. Because ANT is known to alter the energetic state of the cell, these results provoke the idea that understanding the metabolic state of the cell can give further insight into overall cell mechanics, motility, and processes like epithelial-to-mesenchymal transition (EMT). Indeed, others are beginning to find such connections between metabolism and cytoskeletal function (DeWane et al., 2021). By continuing to learn about these connections, we can begin to apply this knowledge to diseases like COPD. We can elucidate more protective phenotypes that ANT may have in the context of cell structure.

Here, *Dictyostelium* was used to understand the feedback between metabolism and cytoskeletal function. With its genetic tractability, rapid growth rate, ease of handling, and genetic homology to mammalian cells, *Dictyostelium* is a suitable model

for studying cellular functions at a fundamental level. Genes responsible for cytokinesis, a significant cell shape change process, have been identified in *Dictyostelium* such as myosin II (*myosin II*; myosin II heavy chain is encoded by *mhcA*), cortexillin I (*cortI*; encoded by *ctxA*), and racE (*racE*) (De Lozanne and Spudich, 1987; Faix et al., 1996; Larochelle et al., 1996; 1997; Manstein et al., 1989). In addition, *Dictyostelium* has been used to study metabolism and as a model for mitochondrial diseases (Pearce et al., 2019). Thus, *Dictyostelium* is an appropriate model to study both cellular mechanics and metabolism. In this study, we optimized assays for *Dictyostelium* and began surveying the relationship of ANT to these cytokinesis/cell mechanic proteins.

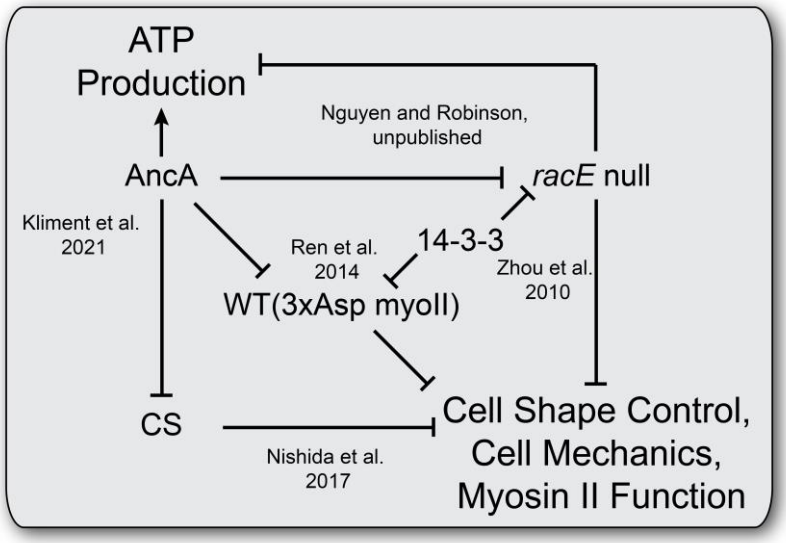

Fig. 4.1. Current understanding between ATP Production, Adenine Nucleotide Translocase (AncA/ANT), and cell shape control and mechanics. ANT overexpression suppresses *racE* nulls (unpublished) and WT(3xAsp myoII) (Ren et al., 2014). In human airway cells, CS also inhibits cell mechanics (Nishida et al., 2017). Our previous studies also linked 14-3-3 to myosin II and racE to control contractility (Zhou et al., 2010). ANT suppresses CS by elevating ATP production and increasing ATP flux (Kliment et al., 2021). Further, *racE* nulls have reduced basal metabolic activity, which produces ATP.

Optimization of the Seahorse mito stress assay for *Dictyostelium*

The Seahorse Flux Analyzer has been widely used to measure metabolic activity in a variety of cell types. Oxygen consumption rate is measured after the injection of

various inhibitors of the electron transport chain, resulting in different metabolic outputs as demonstrated in **Figure 4.2A**. It has been adapted previously for use with *Dictyostelium* in a 24-well format (Lay *et al.*, 2016). We proceeded to adapt this assay for a 96-well format. Because the responses from Antimycin A and Rotenone were not as effective initially, various concentrations of these drugs were used, and their effectiveness was monitored (**Figure 4.2B,C**). The final concentrations ultimately used in subsequent assays are as follows: oligomycin (20 µM), FCCP (10 µM), Antimycin A (30 µM), and Rotenone (30 µM).

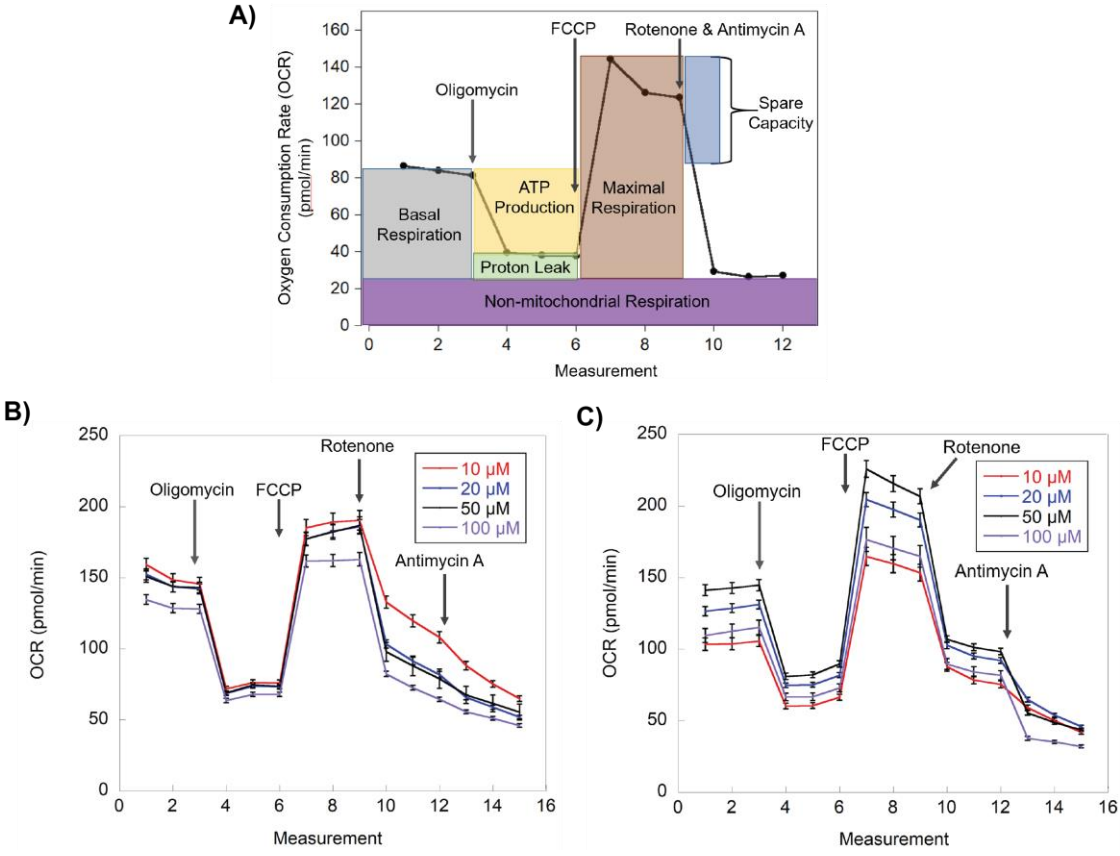

Figure 4.2. Optimization of the Seahorse mito stress test for *Dictyostelium* in a 96-well format. A) The Seahorse Flux Analyzer mito stress test is used to measure metabolic activity through changes in oxygen consumption rate (OCR) after the injection of various inhibitors of the electron transport chain. A range of concentrations for **B)** rotenone and **C)** antimycin A were tested separately in wild-type cells to determine the final concentration to use for subsequent assays. Each curve is representative of n=22-24 wells.

Changes in Cortexillin I expression modulates metabolic activity

With the optimized Seahorse assay, we began monitoring the metabolic activity of cytoskeletal mutants. We began with *cortI* null mutants, and interestingly we observed they had lowered metabolic activity compared to the wild-type strain (**Figure 4.3A**). The *cortI* null cell line was complemented with mCherry-tagged CortI and this interestingly increased metabolic activity to a higher level than WT (**Figure 4.3A**). Basal respiration, ATP production, and spare respiratory capacity were decreased in the *cortI* null cells (**Figure 4.3B,C,D**). Interestingly, when we monitor mitochondrial structures, we did not visually see a difference in mitochondrial distribution between *cortI* null and the rescue cell line. These data so far suggest that CortI is having an influence on metabolic activity, but not through changes in mitochondrial distribution.

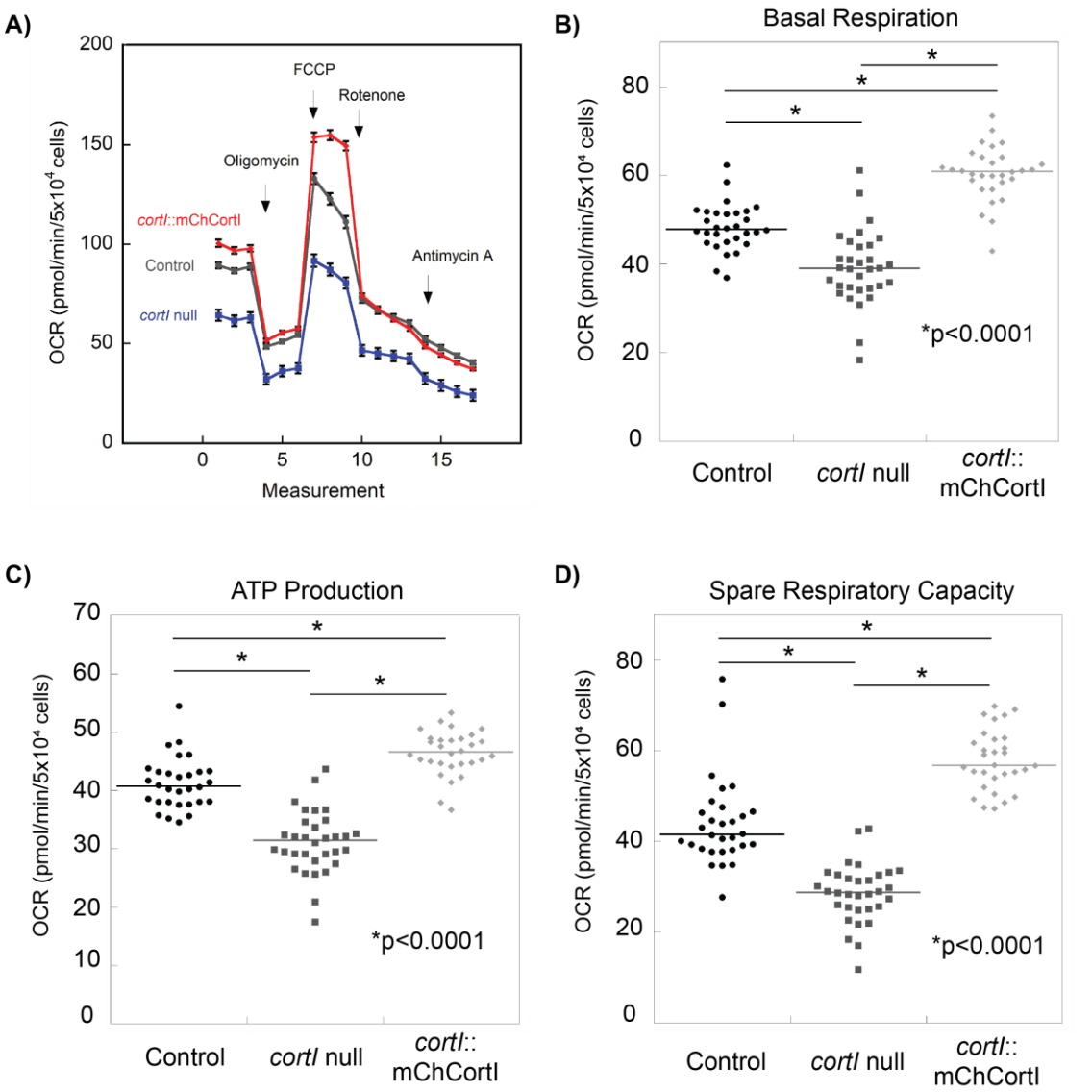

Figure 4.3. *Dictyostelium cortexillin I* null cells have reduced metabolic activity. **A)** The Seahorse Flux Analyzer mito stress test was used to measure differences in oxygen consumption rate (OCR) of wild-type (WT), *cortI* null, and mCherry-CortI complemented *cortI* null *Dictyostelium* cells. The mutants have reduced metabolic activity compared to WT and complementing with mCherry-CortI rescues metabolic function. These metabolic differences are reflected through **B)** basal respiration, **C)** ATP production, and **D)** spare respiratory capacity. n=30-32 wells. Results of Wilcoxon-Mann-Whitney test versus WT. *P*-values are as noted.

Chapter 5: Conclusions

From these studies, we have utilized *Dictyostelium discoideum* as a discovery tool to identify adenine nucleotide translocase (ANT) as protective against cigarette smoke (CS). Evidence suggests that mitochondrial dysfunction is a parameter that arises from CS exposure (Aghapour *et al.*, 2020). Interestingly, we observed through the Seahorse assay that ANT protected metabolic activity in the presence of CS (Kliment *et al.*, 2021). Yet, there was actually an increase in reactive oxygen species (ROS) via MitoSOX after ANT overexpression (Kliment *et al.*, 2021). These results oppose other studies that have suggested that overexpression of ANT protects against oxidative stress in other cell types (Graham et al., 1997). Nonetheless, something to note is that MitoSOX measures mitochondrial superoxide. Mitochondrial superoxide is generated by an increase in mitochondrial membrane permeabilization and the respiration process, which are facilitated by ANT (Marchi et al., 2012; Vieira et al., 2000). Thus, the increase in MitoSOX correlates to an increase in ANT overexpression, but this may not be enough to correspond to an increase in cell death as we discovered in our apoptosis experiments (Kliment *et al.*, 2021).

In addition to metabolism, we interestedly observed that ANT offered protection against CS by modulating mucociliary clearance in the airway epithelium. The airway epithelium is the first line of defense in the lung and acts a barrier to outside toxins. Along the surface of the airway is the airway surface liquid (ASL), an aqueous layer of water and mucus that traps these toxins (Lazarowski *et al.*, 2004). Normal mucociliary transport consists of beating cilia which move the ASL along the airway to carry out trapped pathogens and particulates. CS can disrupt mucociliary transport by decreasing ASL height and ciliary beat frequency (CBF), leading to a build-up of mucus and pathogens that can cause inflammation and lead to COPD phenotypes (Tuder and

Petrache, 2012). Here, we observed that increased expression of ANT increased ASL height, and CBF did not slow down after treatment with CS.

Considering that ANT is canonically a mitochondrial protein, it is interesting that we see it modulate processes such as airway hydration and ciliary function. An important component in mucociliary transport is the signaling pathways initiated by the release of extracellular ATP. A few transporters have been implicated in releasing ATP extracellularly including pannexin-1 (Seminario-Vidal et al., 2011). While ANT could modulate purinergic receptor signaling by increasing ATP production and flux, as we previously found, our data also suggest that ANT could also function as an extracellular ATP transporter. When measuring ASL height, we used two potent inhibitors of ANT, bongkrekic acid (BKA) and carboxyatractyloside (CATR). Both inhibitors prevented the increase in ASL height by ANT overexpression. CATR is a membrane-impermeable inhibitor, suggesting that it acts on ANT that is localizing to the cell surface (Vignais et al., 1973). Our metabolic data also verified that CATR does not work through intracellular ANT, so we proceeded to examine ANT localization in both human lung tissue and differentiated NHBE (Kliment *et al.*, 2021). In both lung tissue and cells, we did observe ANT at the plasma and ciliary membranes through immunofluorescence imaging. We verified that the antibodies used were specific to ANT, which further supported our observations. Interestingly, other studies in hepatocytes and endothelial cells have also identified ectopic ANT, and both ANT1 and ANT2 have predicted secretion-signal sequences that could be the basic of their presence at the plasma membrane (Cardouat et al., 2017; Martinez et al., 2015).

Another interesting avenue of protection that ANT may have is through cell shape change. Airway structure and essential in maintaining normal airway function. Modulators of actin, for instance, are thought to drive epithelial-to-mesenchymal transition (EMT) and airway tissue remodeling (Aghapour *et al.*, 2018; Jiang *et al.*,

2017). We have previously found that continual exposure to CS increases actin assembly and barrier permeability (Nishida *et al.*, 2017). The idea that metabolism and the cytoskeleton interact with each other in a complex feedback system is growing, including through our own studies (DeWane *et al.*, 2021). With the data we have thus far in *Dictyostelium*, we do see some evidence of decreased metabolic activity in cells lacking cytoskeletal proteins. Interestingly, *cortI* null mutants regained metabolic activity after being complemented with Cortexillin I. One hypothesis is that *cortI* mutants might have a less organized cortical actin meshwork, leading to an overall lower energetic state. Future work will be done with ANT overexpression to see if it might alleviate this issue for *cortI* null cells and lead to a partial rescue.

Overall, a tremendous need exists for discovering new core biology and ways to incorporate this into therapeutic development and in a more precision-based approach toward treating patients. The idea of using model organisms to discover new lung biology and studying new biology in human-disease models is especially promising, considering that the current models are concepts that have not changed for about three decades. From this idea, we identified ANT as a modulator of metabolism, ciliary function, airway hydration, and potentially cell shape change in the context of COPD. As mentioned previously, all these parameters are altered in COPD, making ANT a potential therapeutic target. Our discovery of ANT and its protective mechanisms are likely to provide the opportunities for new breakthroughs for COPD and other diseases with similar pathways.

Chapter 6: Future Directions

In the future, there are many directions the COPD and ANT project could take. Our data suggests that ANT is localizing at the cell surface, and we hypothesize that it is contributing to airway hydration by releasing extracellular ATP. To confirm this functionality at the cell membrane, we can measure extracellular ATP with luciferin and luciferase on top of ciliated NHBEs as other groups have done (Seminario-Vidal et al., 2009). ATP concentrations can be measured at steady state at a single time point. ATP release rate can also be measured over time after treatment with a hypotonic solution, which will induce the release of ATP.

We demonstrated that ANT is protective against CS in several ways, making it a potential therapeutic target for COPD. It would be interesting to begin developing a drug screen to probe for therapeutic molecules that can activate ANT or even phenocopy it. To screen for therapeutic molecules that will enhance ANT activity, a new drug library from the ChemCore of the Johns Hopkins Pharmacology and Molecular Sciences department could be used in a phenotypic screen with *Dictyostelium*. *Dictyostelium* will be used because our lab has experience using it to screen for compounds, and the initial genetic selection showed that *Dictyostelium* exposed to CS have hindered cell growth, an easily measurable phenotypic readout (Kliment *et al.*, 2021). Hence, the screen will be based on cell death after exposure to CS. With 96-well plates, wild-type cells will be exposed to 40% CSE, as our preliminary data indicates that ANT is protective at this concentration. Cell survival will be visualized with a nuclear marker. For controls, wells with no cells, wild-type cells, and cells overexpressing AncA (the *Dicty* ortholog of ANT) will be subjected to this assay without drug treatment. The assay will be validated before it will be used with compounds. Compounds of interest from the screen will then be furthered tested with the concept of quantitative phenotypic fingerprinting, which is the identification of compounds based on their ability to induce quantifiable phenotypes that

modulate disease-relevant biology in cells. Essentially, we will observe whether the compounds can induce phenotypes in NHBEs which are characteristic of ANT OE (*e.g.* increase in ASL height, maintaining normal CBF). Compounds that phenocopy ANT OE may be relevant to treating disease because they can reverse CS injury. While the targets of these compounds of interest will be initially unknown, if they induce the same, or similar, quantitative phenotypes across the spectrum of readouts used to identify and characterize ANT OE, this increases the chances that ANT activity is involved. To begin validating whether ANT is a target for our hits, we will use a variety of techniques (*e.g.* western blotting) to see if there are changes in ANT expression after drug treatment. We will also utilize a thermal shift assay in a cellular format, called the cellular thermal shift assay (CETSA), to detect interactions (Jafari et al., 2014). This assay consists of treating cells with drug, collecting cell lysates in tubes, denaturing proteins with heat, and separating precipitated proteins in the pellet fraction from the soluble protein fraction. Both fractions are run on a western and then probed for a target of interest. Proteins that are bound to a drug, potentially ANT in this case, will remain soluble, while those that are not will be in the pellet. Even if ANT is not a target, compounds that phenocopy ANT can still have therapeutic potential since they will elicit protective properties and will not be toxic to human cells. This phenotypic cell process-based screen varies from the traditional target-based drug discovery screen, and we propose the compounds from a cell process-based screen have higher chances of being disease-relevant as a result (**Figure 6.1**).

In terms of the feedback between metabolism and cytoskeletal function, we will continue deciphering the relationship between ANT to the *Dictyostelium* cytoskeletal mutants. This includes performing the Seahorse assay with *racE* null cells, *myoII* null cells, *cortI* null cells, and these mutants with overexpressed ANT. ANT levels will also be probed through western analysis in these mutant lines to see if they affect ANT

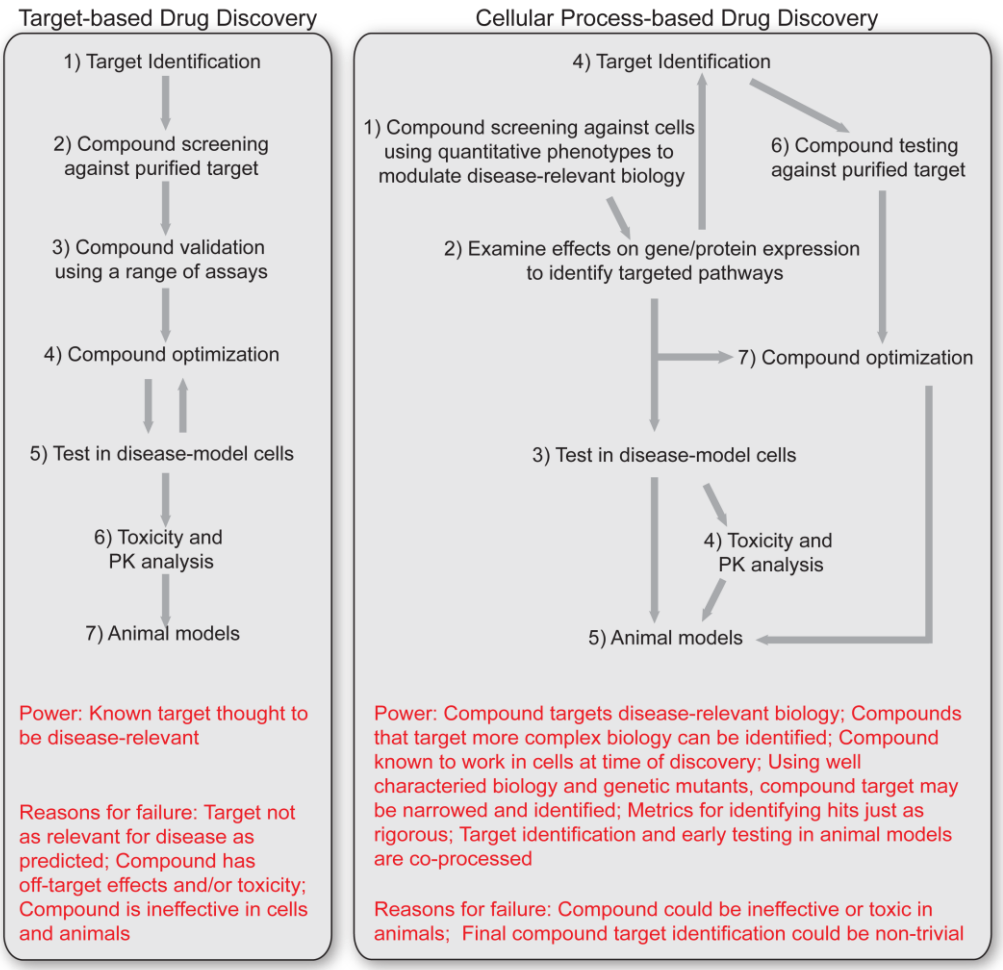

Figure 6.1. Cellular process-based drug discovery versus tradition target-based drug discovery. As opposed to target-based discovery, cellular process-based drug discovery is more focused on identifying quantitative protective phenotypes which are more relevant to disease.

expression. There is evidence that mitochondrial function and dynamics are integrated with cytoskeletal function (DeWane *et al.*, 2021). Thus, we will also observe whether mitochondrial mass and subcellular distribution are altered in these mutants. Mitochondrial dysfunction can also be probed. MitoSOX will be used to observe if there is mitochondrial dysfunction through an increase in reactive oxygen species. The effects of ANT knockdown/inhibition will also be assessed. The impact of ANT depletion on cytokinesis fidelity and cell mechanics will be deciphered through western analysis, micropipette aspiration, compression, and cytokinesis dynamics.

Both the Seahorse assay and mitochondrial assays are useful for gathering information on oxidative phosphorylation. Recently, others have found a connection between the metabolic state and the mechanical state of cells through glycolytic processes. It would be of interest to also consider the impact of glycolysis in our studies. Proteins such as activated AMPK (P-AMPK) and phosphofructose kinase-1 (PFK) are known to be altered in response to mechanical stresses and changes in metabolic activity (DeWane *et al.*, 2021). We could examine the P-AMPK/AMPK ratios and PFK distribution in the cytokinesis mutants. Interestingly, changes in these proteins and glycolysis may be linked back to ANT. Proteins such as AMPK respond to changes in ATP levels, which is contributed by ANT activity. Overall, these experiments will aid in uncovering the impact of ANT on cellular mechanics, which can have future implications of ANT protection in COPD.

Contributions

Corrine Kliment initiated and led the COPD project during her time in the Robinson lab. We both collected data on airway hydration, ciliary beat frequency, human lung tissue IF imaging, and NHBE IF imaging. Pablo Iglesias developed the MatLab scripts for ASL and CBF measurements. Mark Jacob assisted in developing the complemented cytoskeletal mutant cell lines and performing Seahorse assays on them.

This work was supported by the NIH supported by the National Institutes of Health (HL124099, HL151107, GM66817 and F31HL145910).

Bibliography

1. Aghapour, M., Raee, P., Moghaddam, S.J., Hiemstra, P.S., and Heijink, I.H. (2018). Airway Epithelial Barrier Dysfunction in Chronic Obstructive Pulmonary Disease: Role of Cigarette Smoke Exposure. Am J Respir Cell Mol Biol *58*, 157-169. 10.1165/rcmb.2017-0200TR.
2. Aghapour, M., Remels, A.H.V., Pouwels, S.D., Bruder, D., Hiemstra, P.S., Cloonan, S.M., and Heijink, I.H. (2020). Mitochondria: at the crossroads of regulating lung epithelial cell function in chronic obstructive pulmonary disease. Am J Physiol Lung Cell Mol Physiol *318*, L149-L164. 10.1152/ajplung.00329.2019.
3. Alsafadi, H.N., Uhl, F.E., Pineda, R.H., Bailey, K.E., Rojas, M., Wagner, D.E., and Konigshoff, M. (2020). Applications and Approaches for Three-Dimensional Precision-Cut Lung Slices. Disease Modeling and Drug Discovery. Am J Respir Cell Mol Biol *62*, 681-691. 10.1165/rcmb.2019-0276TR.
4. Aravamudan, B., Thompson, M., Sieck, G.C., Vassallo, R., Pabelick, C.M., and Prakash, Y.S. (2017). Functional Effects of Cigarette Smoke-Induced Changes in Airway Smooth Muscle Mitochondrial Morphology. J Cell Physiol *232*, 1053-1068. 10.1002/jcp.25508.
5. Barkauskas, C.E., Chung, M.I., Fioret, B., Gao, X., Katsura, H., and Hogan, B.L. (2017). Lung organoids: current uses and future promise. Development *144*, 986-997. 10.1242/dev.140103.
6. Barnes, P.J. (2016a). Inflammatory mechanisms in patients with chronic obstructive pulmonary disease. J Allergy Clin Immunol *138*, 16-27. 10.1016/j.jaci.2016.05.011.

7. Barnes, P.J. (2016b). Kinases as Novel Therapeutic Targets in Asthma and Chronic Obstructive Pulmonary Disease. Pharmacol Rev *68*, 788-815. 10.1124/pr.116.012518.
8. Barnes, P.J. (2018). Targeting cytokines to treat asthma and chronic obstructive pulmonary disease. Nat Rev Immunol *18*, 454-466. 10.1038/s41577-018-0006-6.
9. Barnes, P.J. (2020). Oxidative stress-based therapeutics in COPD. Redox Biol *33*, 101544. 10.1016/j.redox.2020.101544.
10. Benam, K.H., Villenave, R., Lucchesi, C., Varone, A., Hubeau, C., Lee, H.H., Alves, S.E., Salmon, M., Ferrante, T.C., Weaver, J.C., et al. (2016). Small airway-on-a-chip enables analysis of human lung inflammation and drug responses in vitro. Nat Methods *13*, 151-157. 10.1038/nmeth.3697.
11. Bihlet, A.R., Karsdal, M.A., Sand, J.M., Leeming, D.J., Roberts, M., White, W., and Bowler, R. (2017). Biomarkers of extracellular matrix turnover are associated with emphysema and eosinophilic-bronchitis in COPD. Respir Res *18*, 22. 10.1186/s12931-017-0509-x.
12. Calverley, P.M., Rabe, K.F., Goehring, U.M., Kristiansen, S., Fabbri, L.M., Martinez, F.J., M, and groups, M.s. (2009). Roflumilast in symptomatic chronic obstructive pulmonary disease: two randomised clinical trials. Lancet *374*, 685-694. 10.1016/S0140-6736(09)61255-1.
13. Cardouat, G., Duparc, T., Fried, S., Perret, B., Najib, S., and Martinez, L.O. (2017). Ectopic adenine nucleotide translocase activity controls extracellular ADP levels and regulates the F1-ATPase-mediated HDL endocytosis pathway on hepatocytes. Biochim Biophys Acta Mol Cell Biol Lipids *1862*, 832-841. 10.1016/j.bbalip.2017.05.005.
14. Castaldi, P.J., Guo, F., Qiao, D., Du, F., Naing, Z.Z.C., Li, Y., Pham, B., Mikkelsen, T.S., Cho, M.H., Silverman, E.K., and Zhou, X. (2019). Identification

of Functional Variants in the FAM13A Chronic Obstructive Pulmonary Disease Genome-Wide Association Study Locus by Massively Parallel Reporter Assays. Am J Respir Crit Care Med *199*, 52-61. 10.1164/rccm.201802-0337OC.

15. Charron, C.E., Russell, P., Ito, K., Lea, S., Kizawa, Y., Brindley, C., and Singh, D. (2017). RV568, a narrow-spectrum kinase inhibitor with p38 MAPK-alpha and -gamma selectivity, suppresses COPD inflammation. Eur Respir J *50*. 10.1183/13993003.00188-2017.
16. Cuadrado, A., Rojo, A.I., Wells, G., Hayes, J.D., Cousin, S.P., Rumsey, W.L., Attucks, O.C., Franklin, S., Levonen, A.L., Kensler, T.W., and Dinkova-Kostova, A.T. (2019). Therapeutic targeting of the NRF2 and KEAP1 partnership in chronic diseases. Nat Rev Drug Discov *18*, 295-317. 10.1038/s41573-018-0008-x.
17. D'Anna, C., Cigna, D., Di Sano, C., Di Vincenzo, S., Dino, P., Ferraro, M., Bini, L., Bianchi, L., Di Gaudio, F., Gjomarkaj, M., and Pace, E. (2017). Exposure to cigarette smoke extract and lipopolysaccharide modifies cytoskeleton organization in bronchial epithelial cells. Exp Lung Res *43*, 347-358. 10.1080/01902148.2017.1377784.
18. De Lozanne, A., and Spudich, J.A. (1987). Disruption of the Dictyostelium myosin heavy chain gene by homologous recombination. Science *236*, 1086. 10.1126/science.3576222.
19. De Smet, E.G., Van Eeckhoutte, H.P., Avila Cobos, F., Blomme, E., Verhamme, F.M., Provoost, S., Verleden, S.E., Venken, K., Maes, T., Joos, G.F., et al. (2020). The role of miR-155 in cigarette smoke-induced pulmonary inflammation and COPD. Mucosal Immunol *13*, 423-436. 10.1038/s41385-019-0241-6.
20. DeWane, G., Salvi, A.M., and DeMali, K.A. (2021). Fueling the cytoskeleton - links between cell metabolism and actin remodeling. J Cell Sci *134*. 10.1242/jcs.248385.

21. Dianat, M., Radan, M., Badavi, M., Mard, S.A., Bayati, V., and Ahmadizadeh, M. (2018). Crocin attenuates cigarette smoke-induced lung injury and cardiac dysfunction by anti-oxidative effects: the role of Nrf2 antioxidant system in preventing oxidative stress. Respir Res *19*, 58. 10.1186/s12931-018-0766-3.
22. Effler, J.C., Kee, Y.S., Berk, J.M., Tran, M.N., Iglesias, P.A., and Robinson, D.N. (2006). Mitosis-specific mechanosensing and contractile-protein redistribution control cell shape. Curr Biol *16*, 1962-1967. 10.1016/j.cub.2006.08.027.
23. Faix, J., Steinmetz, M., Boves, H., Kammerer, R.A., Lottspeich, F., Mintert, U., Murphy, J., Stock, A., Aebi, U., and Gerisch, G. (1996). Cortexillins, major determinants of cell shape and size, are actin-bundling proteins with a parallel coiled-coil tail. Cell *86*, 631-642. 10.1016/s0092-8674(00)80136-1.
24. Ghorani, V., Boskabady, M.H., Khazdair, M.R., and Kianmeher, M. (2017). Experimental animal models for COPD: a methodological review. Tob Induc Dis *15*, 25. 10.1186/s12971-017-0130-2.
25. Ghosh, A., Boucher, R.C., and Tarran, R. (2015). Airway hydration and COPD. Cell Mol Life Sci *72*, 3637-3652. 10.1007/s00018-015-1946-7.
26. Global Initiative for Chronic Obstructive Lung Disease. (2020). https://goldcopd.org/wp-content/uploads/2019/11/GOLD-2020-REPORT-ver1.1wms.pdf
27. Graham, B.H., Waymire, K.G., Cottrell, B., Trounce, I.A., MacGregor, G.R., and Wallace, D.C. (1997). A mouse model for mitochondrial myopathy and cardiomyopathy resulting from a deficiency in the heart/muscle isoform of the adenine nucleotide translocator. Nature Genetics *16*, 226-234. 10.1038/ng0797-226.
28. Green, R.M., Gally, F., Keeney, J.G., Alper, S., Gao, B., Han, M., Martin, R.J., Weinberger, A.R., Case, S.R., Minor, M.N., and Chu, H.W. (2009). Impact of

cigarette smoke exposure on innate immunity: a Caenorhabditis elegans model. PLoS One *4*, e6860. 10.1371/journal.pone.0006860.

29. Hanna, J., Hossain, G.S., and Kocerha, J. (2019). The Potential for microRNA Therapeutics and Clinical Research. Front Genet *10*, 478. 10.3389/fgene.2019.00478.
30. Hedstrom, U., Hallgren, O., Oberg, L., DeMicco, A., Vaarala, O., Westergren-Thorsson, G., and Zhou, X. (2018). Bronchial extracellular matrix from COPD patients induces altered gene expression in repopulated primary human bronchial epithelial cells. Sci Rep *8*, 3502. 10.1038/s41598-018-21727-w.
31. Hiemstra, P.S., Tetley, T.D., and Janes, S.M. (2019). Airway and alveolar epithelial cells in culture. Eur Respir J *54*. 10.1183/13993003.00742-2019.
32. Huang, P., Lazarowski, E.R., Tarran, R., Milgram, S.L., Boucher, R.C., and Stutts, M.J. (2001). Compartmentalized autocrine signaling to cystic fibrosis transmembrane conductance regulator at the apical membrane of airway epithelial cells. Proc Natl Acad Sci U S A *98*, 14120-14125. 10.1073/pnas.241318498.
33. Jafari, R., Almqvist, H., Axelsson, H., Ignatushchenko, M., Lundbäck, T., Nordlund, P., and Molina, D.M. (2014). The cellular thermal shift assay for evaluating drug target interactions in cells. Nature Protocols *9*, 2100-2122. 10.1038/nprot.2014.138.
34. Jia, R., Zhang, H., Yang, Z., Zhao, H., Liu, F., Wang, H., Miao, M., Wang, Q., and Liu, Y. (2017). Protective effects of Schisandrin B on cigarette smoke-induced airway injury in mice through Nrf2 pathway. Int Immunopharmacol *53*, 11-16. 10.1016/j.intimp.2017.09.030.
35. Jiang, J.X., Zhang, S.J., Shen, H.J., Guan, Y., Liu, Q., Zhao, W., Jia, Y.L., Shen, J., Yan, X.F., and Xie, Q.M. (2017). Rac1 signaling regulates cigarette smoke-

induced inflammation in the lung via the Erk1/2 MAPK and STAT3 pathways. Biochim Biophys Acta Mol Basis Dis *1863*, 1778-1788. 10.1016/j.bbadis.2017.04.013.

36. Jiao, Z., Chang, J., Li, J., Nie, D., Cui, H., and Guo, D. (2017). Sulforaphane increases Nrf2 expression and protects alveolar epithelial cells against injury caused by cigarette smoke extract. Mol Med Rep *16*, 1241-1247. 10.3892/mmr.2017.6700.
37. Jones, D.T., Taylor, W.R., and Thornton, J.M. (1992). The rapid generation of mutation data matrices from protein sequences. Comput Appl Biosci *8*, 275-282. 10.1093/bioinformatics/8.3.275.
38. Kee, Y.S., Ren, Y., Dorfman, D., Iijima, M., Firtel, R., Iglesias, P.A., and Robinson, D.N. (2012). A mechanosensory system governs myosin II accumulation in dividing cells. Mol Biol Cell *23*, 1510-1523. 10.1091/mbc.E11-07-0601.
39. Kim, H.T., Yin, W., Jin, Y.J., Panza, P., Gunawan, F., Grohmann, B., Buettner, C., Sokol, A.M., Preussner, J., Guenther, S., et al. (2018). Myh10 deficiency leads to defective extracellular matrix remodeling and pulmonary disease. Nat Commun *9*, 4600. 10.1038/s41467-018-06833-7.
40. Kim, V., and Criner, G.J. (2013). Chronic bronchitis and chronic obstructive pulmonary disease. Am J Respir Crit Care Med *187*, 228-237. 10.1164/rccm.201210-1843CI.
41. Kliment, C.R., Nguyen, J.M.K., Kaltreider, M.J., Lu, Y., Claypool, S.M., Radder, J.E., Sciurba, F.C., Zhang, Y., Gregory, A.D., Iglesias, P.A., et al. (2021). Adenine nucleotide translocase regulates airway epithelial metabolism, surface hydration and ciliary function. J Cell Sci *134*. 10.1242/jcs.257162.

42. Kosmider, B., Lin, C.R., Karim, L., Tomar, D., Vlasenko, L., Marchetti, N., Bolla, S., Madesh, M., Criner, G.J., and Bahmed, K. (2019). Mitochondrial dysfunction in human primary alveolar type II cells in emphysema. EBioMedicine *46*, 305-316. 10.1016/j.ebiom.2019.07.063.
43. Koziol-White, C., Johnstone, T.B., Corpuz, M.L., Cao, G., Orfanos, S., Parikh, V., Deeney, B., Tliba, O., Ostrom, R.S., Dainty, I., and Panettieri, R.A., Jr. (2020). Budesonide enhances agonist-induced bronchodilation in human small airways by increasing cAMP production in airway smooth muscle. Am J Physiol Lung Cell Mol Physiol *318*, L345-L355. 10.1152/ajplung.00393.2019.
44. Kretova, M., Sabova, L., Hodny, Z., Bartek, J., Kollarovic, G., Nelson, B.D., Hubackova, S., and Luciakova, K. (2014). TGF-β/NF1/Smad4-mediated suppression of ANT2 contributes to oxidative stress in cellular senescence. Cellular Signalling *26*, 2903-2911. https://doi.org/10.1016/j.cellsig.2014.08.029.
45. Larochelle, D.A., Vithalani, K.K., and De Lozanne, A. (1996). A novel member of the rho family of small GTP-binding proteins is specifically required for cytokinesis. J Cell Biol *133*, 1321-1329. 10.1083/jcb.133.6.1321.
46. Larochelle, D.A., Vithalani, K.K., and De Lozanne, A. (1997). Role of Dictyostelium racE in cytokinesis: mutational analysis and localization studies by use of green fluorescent protein. Molecular biology of the cell *8*, 935-944. 10.1091/mbc.8.5.935.
47. Lay, S., Sanislav, O., Annesley, S.J., and Fisher, P.R. (2016). Mitochondrial Stress Tests Using Seahorse Respirometry on Intact Dictyostelium discoideum Cells. Methods Mol Biol *1407*, 41-61. 10.1007/978-1-4939-3480-5_4.
48. Lazarowski, E.R., Tarran, R., Grubb, B.R., van Heusden, C.A., Okada, S., and Boucher, R.C. (2004). Nucleotide release provides a mechanism for airway

surface liquid homeostasis. J Biol Chem *279*, 36855-36864. 10.1074/jbc.M405367200.

49. Lea, S., Metryka, A., Li, J., Higham, A., Bridgewood, C., Villetti, G., Civelli, M., Facchinetti, F., and Singh, D. (2019). The modulatory effects of the PDE4 inhibitors CHF6001 and roflumilast in alveolar macrophages and lung tissue from COPD patients. Cytokine *123*, 154739. 10.1016/j.cyto.2019.154739.
50. Lee, H., Lee, J., Hong, S.H., Rahman, I., and Yang, S.R. (2018). Inhibition of RAGE Attenuates Cigarette Smoke-Induced Lung Epithelial Cell Damage via RAGE-Mediated Nrf2/DAMP Signaling. Front Pharmacol *9*, 684. 10.3389/fphar.2018.00684.
51. Lee, S., Shen, Z., Robinson, D.N., Briggs, S., and Firtel, R.A. (2010). Involvement of the cytoskeleton in controlling leading-edge function during chemotaxis. Mol Biol Cell *21*, 1810-1824. 10.1091/mbc.E10-01-0009.
52. Liu, G., Betts, C., Cunoosamy, D.M., Åberg, P.M., Hornberg, J.J., Sivars, K.B., and Cohen, T.S. (2019). Use of precision cut lung slices as a translational model for the study of lung biology. Respiratory Research *20*, 162. 10.1186/s12931-019-1131-x.
53. Liu, Y., and Chen, X.J. (2013). Adenine nucleotide translocase, mitochondrial stress, and degenerative cell death. Oxid Med Cell Longev *2013*, 146860. 10.1155/2013/146860.
54. Lopez-Campos, J.L., Tan, W., and Soriano, J.B. (2016). Global burden of COPD. Respirology *21*, 14-23. 10.1111/resp.12660.
55. Manstein, D.J., Titus, M.A., De Lozanne, A., and Spudich, J.A. (1989). Gene replacement in Dictyostelium: generation of myosin null mutants. Embo j *8*, 923-932.

56. Marchi, S., Giorgi, C., Suski, J.M., Agnoletto, C., Bononi, A., Bonora, M., De Marchi, E., Missiroli, S., Patergnani, S., Poletti, F., et al. (2012). Mitochondria-Ros Crosstalk in the Control of Cell Death and Aging. Journal of Signal Transduction *2012*, 329635. 10.1155/2012/329635.
57. Marklew, A.J., Patel, W., Moore, P.J., Tan, C.D., Smith, A.J., Sassano, M.F., Gray, M.A., and Tarran, R. (2019). Cigarette Smoke Exposure Induces Retrograde Trafficking of CFTR to the Endoplasmic Reticulum. Sci Rep *9*, 13655. 10.1038/s41598-019-49544-9.
58. Martinez, L.O., Najib, S., Perret, B., Cabou, C., and Lichtenstein, L. (2015). Ecto-F1-ATPase/P2Y pathways in metabolic and vascular functions of high density lipoproteins. Atherosclerosis *238*, 89-100. 10.1016/j.atherosclerosis.2014.11.017.
59. McElvaney, G., Blackie, S., Morrison, N.J., Wilcox, P.G., Fairbarn, M.S., and Pardy, R.L. (1989). Maximal static respiratory pressures in the normal elderly. Am Rev Respir Dis *139*, 277-281. 10.1164/ajrccm/139.1.277.
60. Moore, P.J., Reidel, B., Ghosh, A., Sesma, J., Kesimer, M., and Tarran, R. (2018). Cigarette smoke modifies and inactivates SPLUNC1, leading to airway dehydration. FASEB J, fj201800345R. 10.1096/fj.201800345R.
61. Moussa, B.A., El-Zaher, A.A., El-Ashrey, M.K., and Fouad, M.A. (2018). Synthesis and molecular docking of new roflumilast analogues as preferential-selective potent PDE-4B inhibitors with improved pharmacokinetic profile. Eur J Med Chem *148*, 477-486. 10.1016/j.ejmech.2018.02.038.
62. Ng-Blichfeldt, J.P., Gosens, R., Dean, C., Griffiths, M., and Hind, M. (2019). Regenerative pharmacology for COPD: breathing new life into old lungs. Thorax *74*, 890-897. 10.1136/thoraxjnl-2018-212630.
63. Nguyen, J.M.K., Robinson, D.N., and Sidhaye, V.K. (2021). Why new biology must be uncovered to advance therapeutic strategies for chronic obstructive

pulmonary disease. Am J Physiol Lung Cell Mol Physiol *320*, L1-L11. 10.1152/ajplung.00367.2020.

64. Nishida, K., Brune, K.A., Putcha, N., Mandke, P., O'Neal, W.K., Shade, D., Srivastava, V., Wang, M., Lam, H., An, S.S., et al. (2017). Cigarette smoke disrupts monolayer integrity by altering epithelial cell-cell adhesion and cortical tension. Am J Physiol Lung Cell Mol Physiol *313*, L581-L591. 10.1152/ajplung.00074.2017.
65. Patel, N.R., Cunoosamy, D.M., Fageras, M., Taib, Z., Asimus, S., Hegelund-Myrback, T., Lundin, S., Pardali, K., Kurian, N., Ersdal, E., et al. (2018). The development of AZD7624 for prevention of exacerbations in COPD: a randomized controlled trial. Int J Chron Obstruct Pulmon Dis *13*, 1009-1019. 10.2147/COPD.S150576.
66. Pearce, X.G., Annesley, S.J., and Fisher, P.R. (2019). The Dictyostelium model for mitochondrial biology and disease. Int J Dev Biol *63*, 497-508. 10.1387/ijdb.190233pf.
67. Phillips, J.E. (2020). Inhaled Phosphodiesterase 4 (PDE4) Inhibitors for Inflammatory Respiratory Diseases. Front Pharmacol *11*, 259. 10.3389/fphar.2020.00259.
68. Posso, S.V., Quesnot, N., Moraes, J.A., Brito-Gitirana, L., Kennedy-Feitosa, E., Barroso, M.V., Porto, L.C., Lanzetti, M., and Valenca, S.S. (2018). AT-RVD1 repairs mouse lung after cigarette smoke-induced emphysema via downregulation of oxidative stress by NRF2/KEAP1 pathway. Int Immunopharmacol *56*, 330-338. 10.1016/j.intimp.2018.01.045.
69. Prange, R., Thiedmann, M., Bhandari, A., Mishra, N., Sinha, A., Hasler, R., Rosenstiel, P., Uliczka, K., Wagner, C., Yildirim, A.O., et al. (2018). A Drosophila model of cigarette smoke induced COPD identifies Nrf2 signaling as an

expedient target for intervention. Aging (Albany NY) *10*, 2122-2135. 10.18632/aging.101536.

70. Ren, Y., West-Foyle, H., Surcel, A., Miller, C., and Robinson, D.N. (2014). Genetic suppression of a phosphomimic myosin II identifies system-level factors that promote myosin II cleavage furrow accumulation. Mol Biol Cell *25*, 4150-4165. 10.1091/mbc.E14-08-1322.
71. Sakkas, L.I., Mavropoulos, A., and Bogdanos, D.P. (2017). Phosphodiesterase 4 Inhibitors in Immune-mediated Diseases: Mode of Action, Clinical Applications, Current and Future Perspectives. Curr Med Chem *24*, 3054-3067. 10.2174/0929867324666170530093902.
72. Schwiebert, E.M., and Zsembery, A. (2003). Extracellular ATP as a signaling molecule for epithelial cells. Biochimica et Biophysica Acta (BBA) - Biomembranes *1615*, 7-32. https://doi.org/10.1016/S0005-2736(03)00210-4.
73. Sekine, T., Hirata, T., Ishikawa, S., Ito, S., Ishimori, K., Matsumura, K., and Muraki, K. (2019). Regulation of NRF2, AP-1 and NF-kappaB by cigarette smoke exposure in three-dimensional human bronchial epithelial cells. J Appl Toxicol *39*, 717-725. 10.1002/jat.3761.
74. Seminario-Vidal, L., Lazarowski, E.R., and Okada, S.F. (2009). Assessment of extracellular ATP concentrations. Methods Mol Biol *574*, 25-36. 10.1007/978-1-60327-321-3_3.
75. Seminario-Vidal, L., Okada, S.F., Sesma, J.I., Kreda, S.M., van Heusden, C.A., Zhu, Y., Jones, L.C., O'Neal, W.K., Penuela, S., Laird, D.W., et al. (2011). Rho signaling regulates pannexin 1-mediated ATP release from airway epithelia. J Biol Chem *286*, 26277-26286. 10.1074/jbc.M111.260562.
76. Shibata, S., Miyake, K., Tateishi, T., Yoshikawa, S., Yamanishi, Y., Miyazaki, Y., Inase, N., and Karasuyama, H. (2018). Basophils trigger emphysema

development in a murine model of COPD through IL-4-mediated generation of MMP-12-producing macrophages. Proc Natl Acad Sci U S A *115*, 13057-13062. 10.1073/pnas.1813927115.

77. Shrestha, J., Razavi Bazaz, S., Aboulkheyr Es, H., Yaghobian Azari, D., Thierry, B., Ebrahimi Warkiani, M., and Ghadiri, M. (2020). Lung-on-a-chip: the future of respiratory disease models and pharmacological studies. Crit Rev Biotechnol *40*, 213-230. 10.1080/07388551.2019.1710458.
78. Sidhaye, V.K., Holbrook, J.T., Burke, A., Sudini, K.R., Sethi, S., Criner, G.J., Fahey, J.W., Berenson, C.S., Jacobs, M.R., Thimmulappa, R., et al. (2019). Compartmentalization of anti-oxidant and anti-inflammatory gene expression in current and former smokers with COPD. Respir Res *20*, 190. 10.1186/s12931-019-1164-1.
79. Sidhaye, V.K., Nishida, K., and Martinez, F.J. (2018). Precision medicine in COPD: where are we and where do we need to go? Eur Respir Rev *27*. 10.1183/16000617.0022-2018.
80. Singh, D., Abbott-Banner, K., Bengtsson, T., and Newman, K. (2018). The short-term bronchodilator effects of the dual phosphodiesterase 3 and 4 inhibitor RPL554 in COPD. Eur Respir J *52*. 10.1183/13993003.01074-2018.
81. Singh, D., Beeh, K.M., Colgan, B., Kornmann, O., Leaker, B., Watz, H., Lucci, G., Geraci, S., Emirova, A., Govoni, M., and Nandeuil, M.A. (2019). Effect of the inhaled PDE4 inhibitor CHF6001 on biomarkers of inflammation in COPD. Respir Res *20*, 180. 10.1186/s12931-019-1142-7.
82. Skronska-Wasek, W., Mutze, K., Baarsma, H.A., Bracke, K.R., Alsafadi, H.N., Lehmann, M., Costa, R., Stornaiuolo, M., Novellino, E., Brusselle, G.G., et al. (2017). Reduced Frizzled Receptor 4 Expression Prevents WNT/beta-Catenin-

driven Alveolar Lung Repair in Chronic Obstructive Pulmonary Disease. Am J Respir Crit Care Med *196*, 172-185. 10.1164/rccm.201605-0904OC.

83. Sun, Z., Li, F., Zhou, X., Chung, K.F., Wang, W., and Wang, J. (2018). Stem cell therapies for chronic obstructive pulmonary disease: current status of pre-clinical studies and clinical trials. J Thorac Dis *10*, 1084-1098. 10.21037/jtd.2018.01.46.
84. Sundar, I.K., Maremanda, K.P., and Rahman, I. (2019). Mitochondrial dysfunction is associated with Miro1 reduction in lung epithelial cells by cigarette smoke. Toxicol Lett *317*, 92-101. 10.1016/j.toxlet.2019.09.022.
85. Surcel, A., Ng, W.P., West-Foyle, H., Zhu, Q., Ren, Y., Avery, L.B., Krenc, A.K., Meyers, D.J., Rock, R.S., Anders, R.A., et al. (2015). Pharmacological activation of myosin II paralogs to correct cell mechanics defects. Proc Natl Acad Sci U S A *112*, 1428-1433. 10.1073/pnas.1412592112.
86. Tuder, R.M., and Petrache, I. (2012). Pathogenesis of chronic obstructive pulmonary disease. J Clin Invest *122*, 2749-2755. 10.1172/JCI60324.
87. van der Toorn, M., Slebos, D.-J., de Bruin, H.G., Leuvenink, H.G., Bakker, S.J.L., Gans, R.O.B., Koëter, G.H., van Oosterhout, A.J.M., and Kauffman, H.F. (2007). Cigarette smoke-induced blockade of the mitochondrial respiratory chain switches lung epithelial cell apoptosis into necrosis. American Journal of Physiology-Lung Cellular and Molecular Physiology *292*, L1211-L1218. 10.1152/ajplung.00291.2006.
88. Vieira, H.L.A., Haouzi, D., El Hamel, C., Jacotot, E., Belzacq, A.S., Brenner, C., and Kroemer, G. (2000). Permeabilization of the mitochondrial inner membrane during apoptosis: impact of the adenine nucleotide translocator. Cell Death & Differentiation *7*, 1146-1154. 10.1038/sj.cdd.4400778.

89. Vignais, P.V., Vignais, P.M., and Defaye, G. (1973). Adenosine diphosphate translocation in mitochondria. Nature of the receptor site for carboxyatractyloside (gummiferin). Biochemistry *12*, 1508-1519. 10.1021/bi00732a007.

90. Wise, R.A., Holbrook, J.T., Criner, G., Sethi, S., Rayapudi, S., Sudini, K.R., Sugar, E.A., Burke, A., Thimmulappa, R., Singh, A., et al. (2016). Lack of Effect of Oral Sulforaphane Administration on Nrf2 Expression in COPD: A Randomized, Double-Blind, Placebo Controlled Trial. PLoS One *11*, e0163716. 10.1371/journal.pone.0163716.

91. Xu, J., Murphy, S.L., Kockanek, K.D., and Arias, E. (2020). Mortality in the United States, 2018. NCHS Data Brief, 1-8.

92. Yanagisawa, H., Hashimoto, M., Minagawa, S., Takasaka, N., Ma, R., Moermans, C., Ito, S., Araya, J., Budelsky, A., Goodsell, A., et al. (2017). Role of IL-17A in murine models of COPD airway disease. Am J Physiol Lung Cell Mol Physiol *312*, L122-L130. 10.1152/ajplung.00301.2016.

93. Zhang, M., Shi, R., Zhang, Y., Shan, H., Zhang, Q., Yang, X., Li, Y., and Zhang, J. (2019). Nix/BNIP3L-dependent mitophagy accounts for airway epithelial cell injury induced by cigarette smoke. J Cell Physiol *234*, 14210-14220. 10.1002/jcp.28117.

94. Zhang, M., Tang, J., Shan, H., Zhang, Q., Yang, X., Zhang, J., and Li, Y. (2018). p66Shc Mediates Mitochondrial Dysfunction Dependent on PKC Activation in Airway Epithelial Cells Induced by Cigarette Smoke. Oxid Med Cell Longev *2018*, 5837123. 10.1155/2018/5837123.

95. Zhou, Q., Kee, Y.-S., Poirier, C.C., Jelinek, C., Osborne, J., Divi, S., Surcel, A., Will, M.E., Eggert, U.S., Müller-Taubenberger, A., et al. (2010). 14-3-3 coordinates microtubules, Rac, and myosin II to control cell mechanics and cytokinesis. Current biology : CB *20*, 1881-1889. 10.1016/j.cub.2010.09.048.

96. Zou, S.C., Pang, L.L., Mao, Q.S., Wu, S.Y., and Xiao, Q.F. (2018). IL-9 exacerbates the development of chronic obstructive pulmonary disease through oxidative stress. Eur Rev Med Pharmacol Sci *22*, 8877-8884. 10.26355/eurrev_201812_16656.

97. Zscheppang, K., Berg, J., Hedtrich, S., Verheyen, L., Wagner, D.E., Suttorp, N., Hippenstiel, S., and Hocke, A.C. (2018). Human Pulmonary 3D Models For Translational Research. Biotechnol J *13*. 10.1002/biot.201700341.

98. Zuo, H., Faiz, A., van den Berge, M., Mudiyanselage, S., Borghuis, T., Timens, W., Nikolaev, V.O., Burgess, J.K., and Schmidt, M. (2020). Cigarette smoke exposure alters phosphodiesterases in human structural lung cells. Am J Physiol Lung Cell Mol Physiol *318*, L59-L64. 10.1152/ajplung.00319.2019.

99. Zuo, H., Han, B., Poppinga, W.J., Ringnalda, L., Kistemaker, L.E.M., Halayko, A.J., Gosens, R., Nikolaev, V.O., and Schmidt, M. (2018). Cigarette smoke up-regulates PDE3 and PDE4 to decrease cAMP in airway cells. Br J Pharmacol *175*, 2988-3006. 10.1111/bph.14347.

Jennifer Nguyen

725 North Wolfe St, Physiology 100, Baltimore, MD 21231
(678)-209-1678
jnguye27@jhmi.edu

EDUCATION

JOHNS HOPKINS UNIVERSITY SCHOOL OF MEDICINE, BALTIMORE, MD **June 2021**
Ph.D. in Pharmacology and Molecular Sciences

MERCER UNIVERSITY, MACON, GA **May 2015**
B.S. in Biochemistry and Molecular Biology
Summa Cum Laude Graduate with Honors
Cumulative GPA: 3.923/4.000

RESEARCH EXPERIENCE

PH.D. CANDIDATE **2015-Present**
Johns Hopkins University School of Medicine, Baltimore, MD
Advisor: Dr. Douglas Robinson, Ph.D.
Deciphering and discovering the feedback between metabolism and cytoskeletal function

UNDERGRADUATE RESEARCH STUDENT **2013-2015**
Mercer University, Macon, GA
Advisor: Dr. David Goode, Ph.D.
Dynamic combinatorial screening for optimal binders of the pentavalent B-Subunit of cholera toxin

UNDERGRADUATE RESEARCH STUDENT **2012-2013**
Mercer University, Macon, GA
Advisor: Dr. Katharine Northcutt, Ph.D.
Sex differences in Fos immunoreactivity in tyrosine hydroxylase-expressing cells during juvenile rat play

PUBLICATIONS

Nguyen, J., Robinson, D., Sidhaye, V. Why New Biology Must Be Uncovered to Advance Therapeutic Strategies for Chronic Obstructive Pulmonary Disease. *American Journal of Physiology-Lung Cellular and Molecular Physiology* 320, L1-L11 (2021).

Nguyen, J., Liu, Y., Nguyen, L., Sidhaye, V., Robinson, D. Discovery and quantitative dissection of cytokinesis using *Dictyostelium discoideum*. Kimmel A. ed. *Methods in Molecular Biology* (2021); In press.

Kliment, C., **Nguyen, J**., Kaltreider, M., Lu, Y., Claypool, S., Radder, J., Sciurba, F., Zhang, Y., Gregory, A., Iglesias, P., Sidhaye, V., Robinson, D. Adenine Nucleotide Translocase regulates airway epithelial homeostasis, mitochondrial metabolism and ciliary function. *Journal of Cell Science* 134, jcs257162 (2021).

Northcutt, K. and **Nguyen, J**. Female Juvenile Play Elicits Fos Expression in Dopaminergic Neurons of the VTA. *Behavioral Neuroscience* 128, 178-86 (2014).

PRESENTATIONS

Oral presentations
European Respiratory Society International Congress **2018**

Thomas L. Petty Aspen Lung Conference **2018**

Poster Presentations
Pharmacology Graduate Program Retreat **2016, 2017, 2018, 2019**
American Society for Cell Biology (ASCB) conference **2017**
American Chemical Society Southeastern Regional Meeting (SERMACS) **2014**
Society for Behavioral Neuroendocrinology (SBN) conference **2013**

AWARDS AND HONORS

Ruth L. Kirschstein Predoctoral Individual National Research Service Award F31 Grant **2019**
Lewis Travel Award Recipient, Johns Hopkins Department of Cell Biology **2018**
Scheinberg Travel Award Recipient, Johns Hopkins Department of Pharmacology **2018**
NSF Graduate Research Fellowship Program Honorable Mention **2017**
Outstanding Biochemistry and Molecular Biology Student Award **2015**
Barry Goldwater Scholarship Honorable Mention **2014**

SERVICE AND LEADERSHIP

Mentor **2017**
Summer Academic Research Experience, JHMI, Baltimore, Maryland

Treasurer **2018**
Pharmacology Student Initiative, JHMI, Baltimore, Maryland

PROFESSIONAL MEMBERSHIPS

American Society for Cell Biology
European Respiratory Society
Biophysical Society